7-24-2013

An integrated clinico-metabolomic model improves prediction of death in sepsis.

Raymond J. Langley

Ephraim L. Tsalik

Jennifer C. van Velkinburgh

Seth W. Glickman

Brandon J. Rice

See next page for additional authors

Recommended Citation

Langley, R. J., Tsalik, E. L., van Velkinburgh, J. C., Glickman, S. W., Rice, B. J., Wang, C., Chen, B., Carin, L., Suarez, A., Mohney, R. P., Freeman, D. H., Wang, M., You, J., Wulff, J., Thompson, J. W., Moseley, M. A., Reisinger, S., Edmonds, B. T., Grinnell, B., Nelson, D. R., Dinwiddie, D. L., Miller, N. A., Saunders, C. J., Soden, S., Rogers, A. J., Gazourian, L., Fredenburgh, L. E., Massaro, A. F., Baron, R. M., Choi, A. M., Corey, G. R., Ginsburg, G. S., Cairns, C. B., Otero, R. M., Fowler, V. G., Rivers, E. P., Woods, C. W., Kingsmore, S. F. An integrated clinico-metabolomic model improves prediction of death in sepsis. *Sci Transl Med* 5, 195-195 (2013).

Published in final edited form as:
Sci Transl Med. 2013 July 24; 5(195): 195ra95. doi:10.1126/scitranslmed.3005893.

An integrated clinico-metabolomic model improves prediction of death in sepsis

Raymond J. Langley[1,2,*], **Ephraim L. Tsalik**[3,4,*], **Jennifer C. van Velkinburgh**[1,*], **Seth W. Glickman**[5,6], **Brandon J. Rice**[1], **Chunping Wang**[7], **Bo Chen**[7], **Lawrence Carin**[7], **Arturo Suarez**[8], **Robert P. Mohney**[9], **Debra H. Freeman**[5], **Mu Wang**[10], **Jinsam You**[10], **Jacob Wulff**[9], **J. Will Thompson**[4], **M. Arthur Moseley**[4], **Stephanie Reisinger**[11], **Brian T. Edmonds**[12], **Brian Grinnell**[12], **David R. Nelson**[12], **Darrell L. Dinwiddie**[1,13,14], **Neil A. Miller**[1,13], **Carol J. Saunders**[13], **Sarah S. Soden**[13], **Angela J. Rogers**[15,16], **Lee Gazourian**[15], **Laura E. Fredenburgh**[15], **Anthony F. Massaro**[15], **Rebecca M. Baron**[15], **Augustine M.K. Choi**[15], **G. Ralph Corey**[5], **Geoffrey S. Ginsburg**[5], **Charles B. Cairns**[6], **Ronny M. Otero**[8], **Vance G. Fowler Jr**[5], **Emanuel P. Rivers**[8], **Christopher W. Woods**[3,4,5], and **Stephen F. Kingsmore**[1,13]

[1]National Center for Genome Resources, Santa Fe, New Mexico 87505, USA

[2]Lovelace Respiratory Research Institute, Department of Respiratory Immunology, Albuquerque, New Mexico 87108, USA

[3]Department of Medicine, Durham Veterans Affairs Medical Center, Durham, North Carolina 27705, USA

[4]Duke Department of Medicine, Durham, North Carolina, 27710, USA

[5]Duke Institute for Genome Sciences and Policy, and Department of Medicine, Duke University School of Medicine, Durham, North Carolina 27710, USA

[6]Department of Emergency Medicine, University of North Carolina School of Medicine, Chapel Hill, North Carolina 27599, USA

[7]Department of Electrical & Computer Engineering, Duke University, Durham, North Carolina 27710, USA

[8]Department of Emergency Medicine, Henry Ford Hospital, Detroit, Michigan 48202, USA

[*]Authors contributed equally.

Author Contributions: Designed experiments: SFK, RJL, RPM, EPR, RMO, VGF, CWW, CBC, LC, MAM, MW, BTE, DRN, BG, GRC. Provided funding: SFK, VGF, EPR, CWW, RMO, AMKC, GSG, ELT. Performed experiments: RJL performed metabolomic, proteomic, predictive modeling analysis, clinical diagnostic analysis, and cross correlation analysis. RPM performed metabolomic analysis. JW and JY provided MS/MS technical expertise for the metabolomic and proteomic assays, respectively. JCvV performed clinical demographic analysis, and helped with patient selection. SR served as a database manager.. Performed clinical analysis and/or patient enrollment: ELT, SWG, AS, DHF, SR, AJR, LG, LEF, AFM, RMB, AMKC, CBC, VGF, EPR, RMO, CWW, SFK. Performed experimental analysis: RJL, SFK. RPM, BJR, JCvV, CW, BC, RPM, MW, JY, JWT, MAM, DLD, NAM, CJS, SSS, AJR. Wrote the manuscript: RJL, SFK, ELT, CWW, CBC, JCvV, GSG.

Competing Interests. BE and CC are consultants for bioMerieux. VGF has received honoraria in the last 3 years from Achaogen, Arpida, Astellas Pharma, Inc., Cubist Pharmaceuticals, Durata, Inhibitex, Leo Pharma, Merck & Co., Inc., Pfizer, Targanta, Theravance, Inc., and Ortho-McNeil. VGF has been a paid consultant for Affinium, Astellas Pharma, Inc., Biosynexus, Novartis, Cubist Pharmaceuticals, Inimex, Merck & Co., Inc., Galderma, Johnson & Johnson, Medicines Company, Novadigm. VGF was chair of the Merck V710 vaccine for *Staphylococcus aureus* Scientific Advisory Committee and is on the Scientific Advisory Board for Affinium. BR owns Illumina stock. RL, SK, BC, LC have been awarded the following patent related to this work: Method for diagnosis of sepsis and risk of death, US 2010/0273207, 10.28, 2010. RJL, SFK, BC, LC have submitted US patent application No. 12/766,882; RJL and SFK have submitted patent application No. 12/54951 related to this work.

Data and Materials: Proteomic data has been deposited at Proteome Commons (http://www.proteomecommons.org/tranche, dataset 75606). CAPSOD metabolomic data have been deposited at MetaboLights (http://www.ebi.ac.uk/metabolights/; Accession numbers xxx and yyy, respectively).

[9]Metabolon Inc., Durham, North Carolina 27713, USA

[10]Monarch Life Sciences, Indianapolis, Indiana 46202, USA

[11]United BioSource Co., Harrisburg, Pennsylvania 17101, USA

[12]Eli Lilly and Company, Indianapolis, Indiana 46285, USA

[13]Center for Pediatric Genomic Medicine, Children's Mercy Hospitals and Clinics, and Department of Pediatrics, University of Missouri-Kansas City School of Medicine, Missouri 64108, USA

[14]Department of Pediatrics, and Clinical Translational Sciences Center, University of New Mexico Health Sciences Center, Albuquerque, New Mexico, 87131, USA

[15]Division of Pulmonary and Critical Care Medicine, Brigham And Women's Hospital, Boston, Massachusetts, 02115, USA

[16]Channing Laboratory, Boston, Massachusetts, 02115, USA

Abstract

Sepsis is a common cause of death, but outcomes in individual patients are difficult to predict. Elucidating the molecular processes that differ between sepsis patients who survive and those who die may permit more appropriate treatments to be deployed. We examined the clinical features, and the plasma metabolome and proteome of patients with and without community-acquired sepsis, upon their arrival at hospital emergency departments and 24 hours later. The metabolomes and proteomes of patients at hospital admittance who would die differed markedly from those who would survive. The different profiles of proteins and metabolites clustered into fatty acid transport and β-oxidation, gluconeogenesis and the citric acid cycle. They differed consistently among several sets of patients, and diverged more as death approached. In contrast, the metabolomes and proteomes of surviving patients with mild sepsis did not differ from survivors with severe sepsis or septic shock. An algorithm derived from clinical features together with measurements of seven metabolites predicted patient survival. This algorithm may help to guide the treatment of individual patients with sepsis.

Introduction

Sepsis is defined as infection resulting in systemic inflammatory response syndrome (SIRS, a combination of non-specific clinical features of inflammation). Sepsis is the tenth leading cause of death in the United States (1, 2). Sepsis mortality has decreased over the past decade as a result of improved treatment protocols, such as potent anti-microbial drugs and early goal directed therapy (EGDT) (3–6). Choice of treatment is based upon the traditional concept of stepwise sepsis progression and corresponding clinical assessments, such as organ hypoperfusion (1, 7). Therapies that are optimized for individual patients and that target specific sepsis mechanisms have been hard to implement due to non-specific clinical presentations, delayed diagnosis, cryptic severity, and a heterogeneous clinical course (8, 9). Patients may arrive at an emergency department with mild clinical manifestations yet rapidly progress to critical illness. Others have benign courses, despite a similar onset of symptoms, suggesting that host factors play an important role in sepsis development and outcome. Given that infections account for over 10 million emergency department visits per year, and sepsis treatment costs $16.7 billion in the United States (1), there exists an urgent need for more timely sepsis diagnosis, characterization, and prognosis, to inform personalized sepsis treatment of the appropriate intensity. Such information could include a choice of oral or intravenous antibiotics and whether to admit the patient to hospital or start

EGDT (3–10). In addition to better sepsis outcomes, these decisions may decrease unnecessary patient stress and improve the efficiency of resource utilization.

Decades of clinical and molecular studies have identified numerous microbial and host perturbations associated with sepsis outcome. Age and co-morbidity, as codified in the Acute Physiology and Chronic Health Evaluation II (APACHE II) score, for example, are determinants of sepsis outcome (11). Others include the severity of clinical signs at presentation, and after initial therapy. Such clinical signs include the number of SIRS criteria met, lactic acid concentrations in the blood, and early development of shock (failure to maintain blood pressure despite adequate hydration) (12–15). Clinical indices, such as APACHE II and the Sequential Organ Failure Assessment (SOFA), combine multiple clinical measurements in an attempt to aggregate the evidence of the heterogeneous organ dysfunctions that can precede poor outcomes (11, 16). A wide variety of host response biomarkers or biomarker panels have also been examined for utility in sepsis diagnosis and prognostic determination but to date, have lacked the sensitivity and specificity to discriminate individual patient prognoses and outcomes (17–22). This is believed to be due, in part, to the underlying heterogeneity of sepsis. In particular, mortality has been difficult to predict as there are many processes that are associated with death from sepsis, such as uncontrolled inflammation, oxidative stress, immune dysfunction, hemodynamic dysfunction, coagulopathy, metabolic dysfunction and genetic predisposition (23).

Comprehensive, integrated analysis of molecular measurements (24) may allow unbiased identification and prioritization of sepsis outcome signals that may be obscured by false discovery cutoffs or over-interpreted by targeted hypothesis testing. In contrast, analyses of multiple clinico-pathologic data sets should reveal multi-dimensional perturbations of causal networks and pathways. Here, we report the results of a prospective, integrated analysis of outcomes in community-acquired sepsis.

Results

Study Design and Clinical Synopsis

1,152 individuals with suspected, community-acquired sepsis (acute infection and ≥2 SIRS criteria) (15) were enrolled prospectively in the emergency departments at three urban, tertiary-care hospitals in the United States between 2005 and 2009 [Community Acquired Pneumonia and Sepsis Outcome Diagnostics (CAPSOD) study, ClinicalTrials.gov NCT00258869] (12, 17, 25). Patients with SIRS criteria but obvious non-infectious diseases were not enrolled (12). Medical history, physical examination, and acute illness scores (APACHE II and SOFA) (11, 16) were recorded at enrollment (t_0) and 24 hours later (t_{24}), and corresponding blood samples were obtained (Fig. 1A). t_0 was the earliest sampling time available for community-acquired sepsis. Sampling at t_0 and t_{24} allowed evaluation of the trajectory of changes after enrollment. Infection status and outcome through day 28 were independently adjudicated by a board-certified clinician, as described (12, 17, 25) (Table S1). Survival/death was the primary outcome. Standard diagnostic tests were supplemented by tests for capillary lactic acid, urinary pneumococcal antigen and, for a subset of patients, PCR of blood for bacterial and fungal DNA (12, 17, 25). Sixty-three percent of the patients included in this analysis were African American. 28-day mortality was low (4.9%) (12). As CAPSOD was an observational study, clinical care was not standardized and was determined by individual providers.

The discovery set of 150 patients (13% of the total CAPSOD cohort) had five groups that reflected conventional concepts of sepsis progression as a pyramid (1,4). The number of subjects was governed by power to test associations with survival/death. Infection status and infectious agent were adjudicated by a study physician prior to the generation of test data

(12). Standard definitions of organ dysfunction and shock were used (12, 26). The five groups were: day 28 sepsis survivors with uncomplicated courses (n=27), sepsis survivors who developed severe sepsis or septic shock by day 3 (n=25 and n=38, respectively), sepsis nonsurvivors (by day 28; n=31), and non-infected patients who exhibited SIRS criteria (SIRS-positive, "ill" controls, presumed septic at enrollment but later determined to have non-infectious reasons for SIRS; n=29) (12). Due to the few deaths from sepsis in the CAPSOD study, that group defined the attributes of the patients selected for the other four groups (Table 1). The non-infected SIRS group had similar rates of clinical progression as did the sepsis groups (day 3 organ dysfunction and shock, and 28-day death), allowing distinction between the disease progression of sepsis and other SIRS-associated acute illnesses (Table 1). Patients within the sepsis groups were also chosen for infections with *Streptococcus pneumoniae* (n=31), *Escherichia coli* (n=16) and *Staphylococcus aureus* (n=27), three common causes of community-acquired sepsis that often differ in the site of infection and rates of progression.

The experimental design included two validation patient sets (Fig. 1A). Firstly, a separate CAPSOD subset of 18 sepsis nonsurvivors and 34 matched sepsis survivors (at t_0 [Vt_0] and t_{24} [Vt_{24}]). Few patients in the sepsis nonsurvivor group were available after selection of the discovery set because of a low death rate due to sepsis or phlebotomy refusal at t_{24}. Therefore, the sepsis survivors chosen for inclusion in the validation set were matched to those of the available sepsis nonsurvivors based on age, race, sex, and enrollment site. The second validation set was from an independent sepsis study (the Brigham and Women's Hospital Registry of Critical Illness cohort [RoCI], approved by the Partners Human Research Committee, protocol # 2008-P-000495) (27). This set had 29 non-infected patients with SIRS, 36 sepsis survivors and 25 sepsis nonsurvivors.

Plasma Metabolomics

Biochemicals in plasma with a mass-to-charge ratio of 100–1000 Da were measured using label-free, liquid and gas chromatography, and mass spectrometry (MS) (28) (Fig. 1B). Of ~4,400 metabolites potentially detectable in human tissues (29), 439 were measured either at t_0 or t_{24}, and 332 were detected both at t_0 and t_{24}. 214 of the biochemicals detected at t_0 and 224 detected at t_{24} were annotated metabolites (Fig. 2A, B). The median relative standard deviation (SD) of repeated MS measurements of standards was 10% after signal intensity normalization to batch medians. Clinical assays of serum creatinine, capillary lactate and serum glucose correlated well with log-transformed normalized plasma MS values (Fig. 2C, D, E), indicating that the MS assays of metabolite levels were semi-quantitative.

Typically, metabolomics measurements in healthy populations exhibit a normal distribution of Z-scores. However, the distribution of Z-scores in the uninfected SIRS group was right-skewed (log-normal) (Fig. 2F). Patients with severe sepsis and those who died had larger Z-scores that were more skewed than the uninfected SIRS control group (Fig. 2F), indicative of greater metabolomic variance. Principal component analysis (PCA) and Bayesian factor analysis (with normalized factor score plots) were utilized to determine the main sources of inter-individual variation in the plasma metabolome. The Bayesian factor analysis [$c_j = By_j + A(s_j \circ z_j) + \varepsilon_j$] correlated metabolite values (y_j) to clinical parameters (c_j) to define their relevance [where B was the relationship between MS data (y_j) and a clinical parameter (c_j), A was random or undefined effects and ε was random noise]. Clinical parameters (c_j) were normalized with zero-mean and standard deviation and plotted on B-matrices. The strength of clinical parameter-metabolite associations increased from t_0 to t_{24} (by PCA and Bayesian factor analysis, Fig. S1), indicating that metabolomic perturbations were increasing at the time of enrollment. Furthermore, in sepsis nonsurvivors, the variance in the plasma metabolome that was explicable on the basis of sepsis outcomes increased as death

approached (Fig. 2G), consistent with a causal association of metabolome changes with death from sepsis. Remaining variance in the plasma metabolome was largely explained by renal function (semi-quantitative; four groups), liver function (binary) and immunosuppressants (binary) (Fig. S1–S2). Overlaid kernel densities and Mahalanobis distances of metabolome values revealed one septic shock patient to be an outlier, and this patient was therefore removed from subsequent metabolomics analyses.

Plasma metabolites that differed between groups were identified by analysis of variance (ANOVA) at t_0 and t_{24}. Variance unrelated to sepsis was controlled by inclusion of renal function and liver disease as fixed effects. Since acute renal dysfunction showed an association with sepsis nonsurvival, this may have resulted in underestimation of differences due to sepsis outcome (Table S2). Remarkably, no metabolite differed significantly between sepsis survivor subgroups (uncomplicated sepsis, day 3 severe sepsis, day 3 septic shock) or between infectious etiologies (*S. pneumoniae*, *S. aureus* or *E. coli*; Fig. S3) at either t_0 or t_{24}. In contrast, plasma concentrations of 49 metabolites differed between the sepsis survivor groups and the uninfected SIRS-positive group at t_0, whereas 42 metabolites differed at t_{24} (Fig. 3A; ANOVA with inclusion of renal and liver function as fixed effects and false discovery rate (FDR) 5%; sepsis survivor subgroups collapsed; Table S3). In all, 63 metabolites differed between sepsis survivors and uninfected patients at either time point. Of these, 60 had concordant direction of change at both time points, indicating a consistent early metabolic response in sepsis survivors (rather than multiphasic; Fig. S4, and Table S3). Sepsis survivors had lower plasma concentrations of citrate, malate, glycerol, glycerol 3-phosphate, phosphate, 21 amino acids and their catabolites, 12 glycerophosphocholine and glycerophosphoethanolamine esters, and 6 carnitine esters compared to uninfected patients (Fig. 3A, Fig. S5–S6, and Table S3). Six acetaminophen catabolites and two androgenic steroids were increased. Notably, lactate, ketone bodies and carnitine were relatively unchanged between sepsis survivors and uninfected patients.

Next, metabolite values in the collapsed sepsis survivor groups were compared with those in the sepsis nonsurvivor group. Seventy six metabolites differed between the sepsis survivor and death groups at t_0, and 128 metabolites at t_{24} (FDR 5%; Fig. 3A; Fig. S5–S6; and Tables S3). The metabolic differences between the sepsis survivor and death groups were also temporally consistent. Thus, 84 metabolites at one time point that were significantly different between those who survived and those who died,, and detected at the other time point, showed a concordant direction of change. However, inter-individual variability in individual metabolite values was high. Nevertheless, the validity of the differences between survivors and nonsurvivors was supported by the finding that many members of biochemical families had the same direction of change: 17 amino acid catabolites, 16 carnitine esters, 11 nucleic acid catabolites, 5 glycolysis and citric acid cycle components (citrate and malate, pyruvate, dihydroxyacetone, phosphate) and 4 free fatty acids were significantly increased in the sepsis nonsurvivor group (by ANOVA; Fig. S5, and Table S3). Seven glycerophospho -choline and -ethanolamine esters were decreased in the sepsis nonsurvivor group, in agreement with previous studies (23, 30–32). Lactate, an established sepsis severity marker, was elevated in the sepsis nonsurvivor group. Carnitine and ketones were unchanged. Given the regulation of metabolism by steroids, it was notable that anabolic steroids were decreased in the sepsis nonsurvivor group whereas cortisone was increased. These changes were consistent with increased exergonic metabolism in sepsis survivors. A clinical correlate of this conclusion was elevated core temperature in sepsis survivors (38.1°C), but not in the sepsis nonsurvivor group (37.4°C) (Table 1), as previously described (12).

Carnitine esters with medium- or short-chain fatty acids and branched-chain amino acids were the most pronounced biochemical groups that differed between the sepsis nonsurvivor group and survivors. It was possible that these accumulated in blood due to renal

dysfunction and not sepsis itself. To explore this hypothesis, we performed a Bayesian factor analysis with stratification by renal function at t_0 (normal estimated glomerular filtration rate, eGFR ≥ 75 mL/min, n = 44; 32–74 mL/min, n = 56) and binary primary groupings (non-infected, uncomplicated sepsis, severe sepsis, septic shock and sepsis nonsurvivor), etiologic agents (*S. aureus, S. pneumoniae, E. coli*), gender, race, liver disease, hepatitis, alcohol abuse and neoplastic disease). Metabolite factor scores ≥ 0.1 or ≤ −0.1 were considered significant. Liver disease, hepatitis and alcohol abuse had substantial overlap, which may reflect unity. Reassuringly, sepsis nonsurvival and liver disease remained the major contributors of metabolome variance (Fig. S7). The metabolic changes associated with the sepsis nonsurvival factor also remained increased with time (Fig. S7). Moreover the association of carnitine esters with sepsis outcomes remained significant (Table S4 and S5). Thus, the changes in carnitine esters were not explained by renal function.

Validation of Metabolomic Findings

Confirmation of the veracity of differences was sought by metabolome profiling of a first validation set [all remaining sepsis nonsurvivors (validation t_0, Vt_0, n=17; Vt_{24}, n=16) and matched sepsis survivors (Vt_0, n=34; Vt_{24}, n=33) (Fig. 1A)]. Samples from two sepsis nonsurvivors and one sepsis survivor were not available at t_{24}; a sample was obtained from one sepsis nonsurvivor who had refused t_0 phlebotomy. It should be noted that the median time-to-death of the validation group was greater than the discovery group (18.5 days *vs.* 10.7 days, respectively), because insufficient sepsis nonsurvivor samples were available for precise matching of discovery and validation sets. Not surprisingly, the metabolic variance attributable to sepsis outcome at Vt_0 was less pronounced than in the t_0 set (Fig. S2). Consequently, less stringent FDRs were applied in ANOVAs for Vt_0 (25%) and Vt_{24} (15%). There were fewer differences and of smaller magnitude between sepsis survivors and nonsurvivors in the validation cohort (18 differences at t_0 and 20 at t_{24}; Fig. 3A, Fig. S5–S6, and Table S3). Nevertheless, the major metabolite differences were recapitulated (elevated amino acid and RNA catabolites, citrate, malate and fatty acids, decreased anabolic steroids and glycerophospho -choline and -ethanolamine esters). The most consistently altered biochemical class in the validation set remained the carnitine esters, with significant increases in 19 of 21 compounds in the sepsis nonsurvivor group for at least one time point.

A second validation study was performed on an independently derived cohort from another institution with a different enrollment protocol (RoCI study). This validation set contained 29 non-infected subjects with SIRS, 36 sepsis survivors, and 25 sepsis nonsurvivors (Table 1). The demographics of RoCI differed from those of the CAPSOD study. A prominent difference was that the principal ethnicity in the RoCI study was Caucasian (78%). Neoplastic disease (75% RoCI *vs.* ~23% CAPSOD) and administration of immunosuppressants (36% RoCI *vs.*6.5–15% CAPSOD) were much higher in the RoCI sepsis nonsurvivor category than found in the sepsis nonsurvivor category for CAPSOD. The metabolome was profiled with identical methods in both studies. ANOVA of the metabolomic results from the RoCI cohort with a 5% FDR recapitulated the CAPSOD study results with regard to alterations in carnitine esters, glycerophospho -choline and -ethanolamine esters, amino acid derivatives, nucleic acid catabolites, glycolysis and citric acid cycle components (representative results presented in Fig. S8; full results to be published by the RoCI group). Furthermore, the direction of change of these analytes recapitulated those of the CAPSOD cohorts, providing strong evidence that these differences reflected sepsis outcomes rather than bias intrinsic to a single study or limited to a single ethnic group.

Further recapitulation of the major findings was sought for eleven representative metabolites by retesting 382 of the CAPSOD discovery and validation samples with targeted,

quantitative assays (Fig. S9–S10, Tables S6, and S7); four samples were not re-assayed for 4-methyl-2-oxopentanoate, 1-linoleoylglycerophosphocholine, 1-archidonoylglycerophosphocholine, 3-(4-hydroxyphenyl) lactate (HPLA), 3-methoxytyrosine, n-acetylthreonine, and pseudouridine because further aliquots were unavailable. The quantitative results correlated with the semi-quantitative MS screening data (correlation coefficients ranging from +0.57 to +0.99) (Fig. S11). While inter-individual variability of the concentrations of the 11 metabolites among subjects was considerable, the previously described differences between sepsis survivors, sepsis nonsurvivors and uninfected SIRS patients were confirmed (Fig. 3B–E and Fig. S12). The average differences in metabolite values between sepsis survivors and nonsurvivors using the quantitative assays were also examined as a function of time to death. The death-survivor differences increased inversely with time-to-death, suggesting temporal correlations of the 11 metabolites with sepsis nonsurvival (Fig. S13).

Plasma Proteomics

A complementary survey of host response in sepsis survival and death was performed by proteome profiling of the 150 subjects in the CAPSOD discovery group (Fig. 1). Plasma proteins identified by MS with high confidence were quantified using two methods: log-transformed quantile-normalized areas-under-the-curve (AUC) of aligned chromatograms after background noise removal (33), and spectral counting. We note that the sensitivity of MS is too low to detect most changes in cytokines and confidence in identities is low as typically only one peptide is detected (34).

Following immunodepletion of abundant plasma proteins (33), 195 and 117 proteins identified with high confidence were measured by the two methods described above, respectively, of which 101 were detected by both methods (Table S8). For proteins with spectral counts >10, measurements derived from the two methods correlated well (Table S8). Clinical assays of serum C reactive protein (CRP) and albumin correlated with log-transformed MS values in plasma (Fig. S14), indicating MS to be at least semi-quantitative. As observed for the metabolome, sepsis group membership explained part of the variation in the plasma proteome (Fig. S15). Other categorical traits that explained variance were liver disease, immunosuppressant agents, and malignancy (Fig. S15). As with the metabolome, only a single significant protein difference was found among sepsis survivor subgroups or between infectious etiologies (Fig. S16). The concentrations of 16 plasma proteins differed between sepsis survivors and uninfected SIRS patients at t_0, and 40 proteins differed at t_{24} (ANOVA with FDR of 5% and with control of non-sepsis-related effects by inclusion of liver disease, immunosuppressants and malignancy as fixed effects) (Table S8). In agreement with previous reports, many inflammatory markers were elevated in sepsis (e.g., CRP, lipopolysaccharide binding protein, leucine-rich α2 glycoprotein, serpin peptidase inhibitor 3, serum amyloid A1 and A3, and selenoprotein P (Table S8) (35, 36). Serpin peptidase inhibitor 1, which inhibits plasmin and thrombin, was increased in sepsis, consistent with previous reports (37, 38). Notably, several thrombolytic proteins (factor XII, plasminogen, kininogen 1 and fibronectin 1) were decreased in sepsis.

Like the metabolome, the plasma proteome disclosed a markedly different host response in sepsis survivors and nonsurvivors (with 56 and 27 significant protein differences at t_0 and t_{24}, respectively; Table S9). There was strong concordance in protein differences at both time points: 44 of 59 plasma proteins with significant survivor-death differences had congruent changes at the other time point. Notable protein families exhibiting differences were complement components (22 of which were increased in the sepsis nonsurvivor group), thrombolytic proteins (8 of which were decreased and 3 increased in the sepsis nonsurvivor group), and fatty acid transport proteins (9 of which were increased in the sepsis nonsurvivor

group; apolipoproteins AI, AII, AIV, L1, CIV, transthyretin, hemopexin, afamin and α -2-HS-glycoprotein; Fig. 4A and Table S9).

Integration of Proteomic and Metabolomic Datasets

We reasoned that true positive changes in the metabolome should be reflected by analogous changes in the proteome. In particular, this should be true for plasma proteomic and metabolomic measurements in the same biochemical pathway. For example, they should recapitulate known substrate-enzyme-product reaction models and members of known biochemical families should co-cluster. Further, we reasoned that it may be possible to impute the class membership of unknown metabolites, familial enzyme pathways, and novel enzymatic reaction models by integration of the proteomic and metabolomic datasets. To explore this, we performed a global cross-correlation and hierarchal clustering of matched metabolites (e.g., t_0 metabolome vs. t_{24} metabolome), or proteins (e.g., t_0 proteome vs. t_{24} proteome) for the 150 discovery subjects. Further, to assess recapitulation of known metabolome-proteome reaction models, we performed cross-correlation and clustering of metabolites with proteins at each time point (e.g., t_0 proteins vs. t_0 metabolites) in the same samples.

The metabolome-metabolome cross-correlation and hierarchal clustering did largely recapitulate known metabolite/biochemical class membership (Fig. 4B): For example, 7 carnitines esters were nearest neighbors at t_0, as were 5 androgenic steroids, 11 glycerophospho -choline and -ethanolamine esters, 5 bile acids, 16 fatty acids, and 12 amino acid metabolites and energy metabolic derivatives (lactate, citrate, glycerol, pyruvate, oxaloacetate) (Fig. 4B, Fig. S17). Furthermore, co-clustering suggested class membership for several unannotated biochemicals. Several of these were confirmed by subsequent structural determination: Unannotated biochemicals X-11302, X-11245 and X-11445, which co-clustered with DHEAS, androsterone sulfate and epiandrosterone sulfate, were determined to be sulfated pregnenolone-related steroids (pregnen-steroid monosulfate, pregnen-diol disulfate and 5α-pregnan-3β, 20α-diol disulfate, respectively); unannotated biochemical X-11421 co-clustered with 8 medium chain acyl-carnitines and was determined to be 4-*cis*-decenoylcarnitine; X-12465 co-clustered with acetyl- and propionyl-carnitine and was determined to be 3-hydroxybutyrylcarnitine (Fig 4B, Fig. S17). Likewise, many functionally or structurally related proteins co-clustered, such as 4 hemoglobin isoforms, 9 complement components, and 10 apolipoproteins (Fig. 4C).

In addition, plasma proteome-metabolome correlations recapitulated a number of known metabolic reaction models. 4,105 of 53,784 plasma protein–metabolite correlations were concordant at t_0 and t_{24} and statistically significant (Bonferroni-corrected $\log_{10}$ p-value<-6.03; Table S10). These included known mass action kinetic models of catalysis or physicochemical complex assembly: Ribonuclease A1 correlated with 12 downstream products of its action (N6-carbamoylthreonyladenosine, N2,N2-dimethylguanosine, pseudouridine, arabitol, arabinose, erythritol, erythronate, gulono-1,4-lactone, allantoin, phosphate, xylonate and xylose). Hemoglobin subunits α1, β, δ and ζ correlated with the component heme, allosteric effector adenosine-5-monophosphate and degradation product xanthine. Subunit D of succinate dehydrogenase (a high confidence protein identification supported by a single peptide) correlated with 3 downstream citric acid cycle intermediates (L-malate, oxaloacetate and citrate; Fig. 4D and Table S11). Several carnitine esters and fatty acids correlated with plasma transporter fatty acid binding proteins (FABP1 and FABP4, Fig. S18 and Table S11). Two fatty acid substrates correlated inversely with Acyl-CoA Synthetase Mitochondrial-like 6 (ACSM6, another high confidence protein identification supported by a single peptide), which catalyzes attachment of fatty acids to CoA for β-oxidation (Fig. S19 and Table S11).

We reasoned that co-cluster hierarchies and correlations might suggest novel enzymatic reaction models. Thus, for example, subunit D of succinate dehydrogenase correlated with pyruvate, lactate and acetyl-carnitine, and may suggest novel regulation of the citric acid cycle (Fig. 4D), which has animal model support (39). Another plausible model was suggested by correlations of ACSM6 with 9 carnitine esters (Fig. S18). ACSM6 acts upstream of carnitine esterification, and mediates mitochondrial fatty acid import. Overall, these analyses served to validate the accuracy of the metabolomic and proteomic measurements.

Derivation and Testing of Outcome Predictive Biomarker Panels

In light of the consistency of the metabolome and proteome changes between sepsis survivors and nonsurvivors, a biomarker panel was developed and assessed for utility in prediction of sepsis outcomes upon arrival at the emergency room (t_0). Four clinical factors (age, mean arterial pressure, hematocrit and temperature) and 12 metabolites (2-methylbutyroylcarnitine, 4-cis-decenoylcarnitine, butyroylcarnitine, hexanoylcarnitine, 4-methyl-2-oxopentanoate, 1-arachidonoylglycerophosphocholine, 1-linoleoylglycerophosphocholine, HPLA, 3-methoxytyrosine, n-acetylthreonine, pseudouridine and lactate) were nominated either by prior clinical analyses (12), or by selection of the most significantly different metabolomic differences in sepsis survivors and deaths by ANOVA and Bayesian factor analysis. These biomarkers were also selected for relevance to the molecular mechanisms suggested for sepsis survival and death. Proteomic biomarkers were not utilized in this analysis. These biomarkers were used to develop a sparse panel for prediction of sepsis outcomes with logistic regression. The number of biomarkers in the panel was reduced to seven by penalized predictor reduction (a statistical method that applies a penalty to the sum of squares of the coefficients to reduce the number of factors; we utilized a maximum of 10 effects, a $\log_{10}$ regularization parameter and a maximum of 5 categories). These were 4-cis-decenoylcarnitine, 2-methylbutyroylcarnitine, butyroylcarnitine, hexanoylcarnitine, lactate, age, and hematocrit. The resultant logistic regression model performed very well for prediction of sepsis outcomes at t_0 in the discovery cohort (AUC 0.847 and accuracy 85.1%). The prognostic utility of the model was also good in the discovery t_{24} dataset, and the validation Vt_0, and Vt_{24} datasets (Table 2). Indeed, the model predicted sepsis nonsurvival or survival better than widely used clinical scores, such as SOFA (score ≥ 7), APACHE II (score ≥ 25), and capillary lactate (≥ 4.0 mg/dL) (Table 2). Since the discovery and validation studies utilized cohorts from the CAPSOD study, it was possible that the model was over-fitted. Therefore, utility of the model was examined in an independently derived sepsis cohort from another institution and with separate metabolic measurements (RoCI) (27). ANOVA showed nine of the 12 biomarker metabolites to have a statistically significant change in sepsis survivors versus nonsurvivors in the RoCI cohort, and all 12 followed the same trends as in the CAPSOD samples (FDR 5%, Fig. S8). The biomarker panel also had strong predictive discrimination between sepsis survival and death in the RoCI cohort (Table 2).

The data generated in the global metabolomics studies were semi-quantitative. To further examine the prognostic utility of the logistic regression model, specific, quantitative MS assays were developed for four of the biomarker metabolites (4-cis-decenoylcarnitine, 2-methylbutyroylcarnitine, butyroylcarnitine and hexanoylcarnitine). The prognostic utility of the biomarker panel was then retested with quantitative clinical values (age, lactic acid and hematocrit) and values from the specific metabolite assays in all samples from the CAPSOD discovery and validation cohorts (93 sepsis nonsurvivors and 235 sepsis survivors). Missing clinical measurements of lactate were imputed from the values obtained from semi-quantitative metabolome methods. Predictive performance was similar to that with the semi-

quantitative assays (Table 2). Such recapitulation was important because quantitative, homogeneous assays would be used for a clinical prognostic test using these biomarkers.

Support vector machine (SVM) learning performs two-group classification that allows expansion of the solution vector on support vectors, extends the solution surfaces from linear to non-linear and allows for errors in the training set (40). SVM learning typically yields biomarker panels with superior performance to other methods. SVM was used to develop a weighted model for prediction of sepsis survival and death using quantitative measurements of the seven biomarkers. Data from 173 unique sepsis survivors and nonsurvivors were used. When values from the same person were available at both t_0 and t_{24}, one sample was randomly selected. This yielded 87 subjects for training and 86 for testing. Values were normalized by subtracting means and dividing by standard deviations. 100 random partitions were performed for training and test data for each setting. The AUC of the SVM model in the test subjects was 0.74 and accuracy was 74.6% (55% for 28-day sepsis nonsurvival and 83.6% for sepsis survival; Table 2).

Discussion

This study sought to characterize and integrate the metabolome, proteome and clinical variables in sepsis survival and death. Somewhat unexpectedly, this analysis delineated differences in host responses to sepsis in survivors and nonsurvivors that were robust and reproducible. As a consequence, the analytes and pathways that differentiate sepsis survival and death hold promise as potential prognostic biomarkers and may also be useful as targets for the development of new therapies for patients at higher risk of death. Prognostic markers of sepsis outcomes have been sought for decades. Prior candidate biomarker studies, while valuable, have had limited clinical prognostic utility, perhaps because of the heterogeneity and complexity of sepsis outcomes. The integrative approach described herein was based on three assumptions. Firstly, a comprehensive, hypothesis-agnostic description of the molecular antecedents to sepsis survival and death would yield new, unbiased insights. Secondly, that integration of clinical, metabolomic and proteomic data might identify signals that were undetected or obscured by false discovery cutoffs in one-dimensional datasets. Thirdly, that analysis of the co-occurrence and correlations of molecular networks and pathways in complementary datasets would further identify and prioritize likely causal molecular mechanisms. Within the statistically significant group differences common to the discovery and replication cohorts, findings were further prioritized by: 1) assembly into networks, pathways or biochemical families; 2) temporal correlations with clinical status; 3) corroboration of *bona fide* networks and pathways by occurrence in complementary datasets; and 4) by cross correlations, hierarchical co-clustering and assembly of mass action kinetic models of catalysis or physicochemical complexes. Finally, prognostic biomarker candidates were chosen to reflect potential underlying molecular mechanisms, rather than the ability to partition accurately.

The integrated, comprehensive analysis of host responses to sepsis revealed a complex, heterogeneous and highly dynamic pathologic state and yielded new insights into molecular mechanisms of sepsis survival or death that may enable outcome prediction and individualized patient treatment. There were both negative and positive findings regarding the pathophysiology of sepsis. A major negative finding was that the plasma metabolome and proteome did not differ between sepsis survivors, severe sepsis survivors, and septic shock survivors. Another negative finding was that there were no major differences between patients with infections with *S. pneumoniae*, *S. aureus* or *E. coli*. These negative findings may reflect heterogeneous patient responses, diverse co-morbidities, sites of infection, or severity of infections within the 3-day window we focused on. It is also possible that changes were overwhelmed by a generalized septic response, and therefore difficult to

detect. Instead, sepsis survivors appeared to represent a molecular continuum, irrespective of progression to severe sepsis or septic shock or class of infective agent. One caveat to this conclusion is that MS-based proteome analysis was insensitive for measurement of low abundance proteins (34), such as cytokines, which are known to differ between etiologic agents (41). Importantly, our study did not support the popular concept that the clinical stages of sepsis progression (uncomplicated sepsis, severe sepsis, and septic shock) reflect host molecular progression (23). Instead, the homogeneity of the metabolome and proteome in the uncomplicated sepsis, severe sepsis, and septic shock groups was remarkable, challenging the traditional notion of a molecular pyramid of sepsis progression (16). While surprising, the absence of substantive molecular differentiation of these clinical states does not negate the importance of early achievement of effective compartmental concentrations of appropriate antibiotics or the known differences in mortality between etiologic agents and sites of infection (3, 4, 42).

The major positive finding in this study was that a majority of host molecular responses were altered antithetically in sepsis survivors and nonsurvivors, when compared to uninfected patients with SIRS criteria. This was evident at time of presentation, increased at t_{24} and became more pronounced as time-to-death decreased. It was observed both in the plasma metabolome and proteome. It was observed in comparisons of mean values of individual analytes, after inclusion of renal and hepatic diseases as fixed effects, and globally, as assessed by variance components and global cross-correlations. Divergent host responses were highly conserved temporally at the level of individual analyte classes, networks and pathways. Thus, there exists a reproducible dichotomy in host molecular responses to sepsis, suggesting molecular allostasis in survivors, and maladaption in non-survivors.

Alterations in fatty acid metabolism were prominent components of the disparate metabolomic phenotype of sepsis survival and death. Plasma concentrations of 6 carnitine esters were decreased in sepsis survivors, relative to controls. In addition, 16 carnitine esters and 4 fatty acids were elevated in sepsis nonsurvivors, relative to controls. These findings were not explicable on the basis of unchanged ratios of free to acylated carnitine or free to protein-bound ratios of fatty acids. Thus, free carnitine concentrations were unchanged. Nine fatty acid transport proteins were decreased in sepsis nonsurvivors, whereas plasma concentrations of two fatty acid binding proteins were increased in sepsisnonsurvivors. While some of these findings have been previously reported (43), together they suggest a profound defect in fatty acid β-oxidation in sepsis nonsurvivors that was absent in sepsis survivors. The rate limiting step in β-oxidation is fatty acid transport from the cytoplasm into the mitochondrial matrix (44). Since the mitochondrial membrane is impermeable to acyl-CoA, the carnitine palmitoyltransferase (CPT; EC 2.3.1.21) enzyme system, in conjunction with acyl-CoA synthetase and carnitine/acylcarnitine translocase, is utilized to shuttle long-chain fatty acids across the mitochondrial membrane, in the form of acyl-carnitines. CPT I is located in the mitochondrial outer membrane, whereas CPT II is in the inner mitochondrial membrane. Transport across the mitochondrial membrane is reversible. Thus, acyl-carnitines that are not utilized for energy production in fatty acid β-oxidation may be reverse transported from mitochondria to the cytoplasm and then into the plasma, where they are excreted (44). Plasma values of acyl-carnitines of all fatty acid lengths were elevated in sepsis nonsurvivors, and were not explained by differences in renal function, suggesting that the metabolic defect in fatty acid β-oxidation occurs at the level of the carnitine shuttle.

Mitochondrial fatty acid β-oxidation in the mitochondrion is accomplished by several acyl-CoA dehydrogenases. Each acyl-CoA dehydrogenase acts on fatty acids of a particular chain length and with a specific degree of branching (44). Acyl-CoA dehydrogenase deficiencies

are characterized by accumulation of fatty acids of the corresponding range of chain lengths. A potentially causal role for elevated carnitine esters in sepsis nonsurvival is suggested by the finding that micromolar amounts cause ventricular dysfunction (45). Furthermore, patients with mutations in medium-chain acyl-CoA dehydrogenase (MCAD) have high rates of sudden death (46). Animal models have shown that MCAD and CPT I are decreased in heart, liver and kidney in sepsis, and are regulated by decreased expression of peroxisome proliferator-activated receptors (PPAR) α, β and δ (43, 47–49). Interestingly, sepsis survival in mouse models improved with PPAR-agonist treatment (50, 51). In addition, PPARs regulate expression of medium-chain acyl-CoA dehydrogenase (52) and fatty acid β-oxidation (53). Furthermore, PPARα expression is decreased in septic shock and correlates with severity (54). While clinically untested, these results suggest that treatment of selected patients with PPAR agonists may improve sepsis outcomes through increased β-oxidation in heart, liver and kidney tissues. As this study focused on patients with sepsis, it remains unclear if elevations in carnitine esters are unique to sepsis nonsurvival or are a broad prognostic biomarker in critical illness. Hypoxia can also lead to increased plasma acyl-carnitines (55), suggesting they may be a non-specific signal of mitochondrial dysfunction. A prospective metabolomic study of critical illness outcomes absent an infection as well as animal/cell culture models of hypoxia and sepsis may provide a better understanding of the specificity of these biomarkers in death.

In stark contrast to increased carnitine esters and free fatty acids in sepsis nonsurvivors was a consistent decrease in glycerophospho -choline and -ethanolamine esters in sepsis survivors and nonsurvivors compared to non-infected patients with SIRS. The changes were consistent with published findings that glycerophospho -choline and -ethanolamine esters were predictive of sepsis mortality (32). Further, it has been suggested that these changes in lipid metabolism reflect decreases in PPARα (43, 49). Interestingly, exogenous stearoylglycerophosphocholine improves outcomes in septic mice (56). Whereas free fatty acid supplementation has not proven effective in a clinical trial of acute lung injury (57), it is unknown if outcomes would be improved by stearoylglycerophosphocholine supplementation.

Glycolysis, gluconeogenesis and the citric acid cycle differed prominently between sepsis survivors and nonsurvivors. Plasma values of citrate, malate, glycerol, glycerol 3-phosphate, phosphate and glucogenic and ketogenic amino acids were decreased in sepsis survivors, relative to controls. In contrast, citrate, malate, pyruvate, dihydroxyacetone, lactate, phosphate and gluconeogenic amino acids were increased in sepsis nonsurvivors. A corroborating proteomic change was found for succinate dehydrogenase, whose concentration correlated with downstream citric acid cycle metabolites malate, oxaloacetate and citrate and with lactate, pyruvate and acetyl-carnitine. A parsimonious explanation of these findings is that sepsis survivors mobilized various energetic substrates and utilized these completely in aerobic catabolism resulting in decreased plasma concentrations, whereas sepsis patients who would ultimately die failed to utilize these fully, displaying elevated concentrations even at the earliest time points evaluated. Significantly lower core temperature in sepsis nonsurvivors versus survivors may be a correlate of poor aerobic catabolism in dying patients (12).

Several other lines of evidence support the hypothesis that mitochondrial function is a major determinant of sepsis outcome. Structural studies show mitochondrial derangements, decreased mitochondrial number and reduced substrate utilization in sepsis nonsurvival, and a progressive drop in total body oxygen consumption occurs as sepsis severity increases (58–65). Further, circulating mitochondrial damage-associated molecular patterns can activate the innate immune response leading to neutrophil-mediated organ injury (66). Recent evidence indicates that increased succinate, a TCA cycle intermediate metabolite, is

an inflammatory signal that can induce IL-1β production in bone marrow derived macrophages (67). Substantive literature demonstrates that an early indicator of sepsis outcomes is mitochondrial biogenesis, (23, 30, 58, 59, 68–72), another PPAR-regulated phenomenon (73). Finally, sepsis-induced multiple organ failure has been noted to occur despite minimal cell death and patient recovery from organ failure is rapid in survivors, indicating that mitochondrial damage in sepsis survivors is reversible (23, 30, 46, 71, 74).

In summary, an integrated analysis revealed quite different host molecular responses to sepsis in patients who would survive and those who would die. In contrast, we found no metabolomic or proteomic differences between sepsis caused by *Streptococcus pneumoniae*, *Escherichia coli* or *Staphylococcus aureus*. It will be interesting to ascertain whether the sepsis nonsurvival profile is recapitulated in other sepsis etiologies or in other SIRS-inducing conditions (60, 75, 76).

Finally, biomarker models were developed to aid in the prediction of sepsis outcomes that were based on these molecular findings. For ease of assay development for clinical utility, a homogeneous biomarker panel was developed, rather than heterogeneous combinations of protein and metabolite markers. In general, previous sepsis biomarker panels have shown disappointing external validation. Reasons may include data over-fitting, reliance on cross-validation rather than independent validation, and recruitment at single sites. We sought to reduce the impact of these limitations by developing sparse panels, recruitment at three sites, selecting metabolites that had a high probability of representing molecular mechanisms, use of two metabolite measurement techniques, and validation both in a separate CAPSOD test set as well as in an independent cohort. A logistic regression model utilizing carnitine esters and clinical variables consistently categorized survivors with greater than 85% accuracy, while sepsis nonsurvivors were accurately predicted with 45 to 55% accuracy in most of the test sets. This model performed better than capillary lactate, SOFA or APACHE II scores. It should be noted that prognostic performance was evaluated in patients at time of presentation at an emergency department. The differences between survivors and non-survivors increased as time-to-death decreased. Thus, serial testing of sepsis patients may better differentiate those with poor outcomes. Thus, as with many current disease severity markers, this panel is likely to be especially useful when used serially in individual patients. Ideally, the panel would be deployed on a device that performs at point-of-care or hospital-based and with rapid time-to-result. The biomarkers presented here were the best performing models but are by no means the only variables with such predictive utility. Independent replication studies are needed, as are finalization of markers, normalized time-to-death analysis, and additional assay development.

One concern for a model predicting survival or death is that subsequent clinical decision making may be biased in a way that supports the prediction, resulting in considerable risk of harm. However, results in animal models targeting glycerophosphocholine esters and PPAR expression suggest that mechanisms can be reversed and outcomes improved by targeted treatments that improve β-oxidation and/or neutrophil-mediated bacterial killing (50, 51, 53, 56). Additionally, preliminary findings were that sepsis survivors after EGDT had higher levels of carnitine esters at presentation than sepsis survivors who did not receive EGDT, further suggesting that metabolic and mitochondrial dysfunction can be mitigated. Therapeutic targets that were nominated by this study include glycerophospho -choline and -ethanolamine esters, acetylcarnitine supplementation, PPAR agonist treatment, inhibition of the γ-aminobutyric shunt, or enhancement of mitochondrial biogenesis (10, 39, 50, 51, 56, 67). Upon additional development, a sepsis prognosis panel may aid in the immense need for individualization of the intensity of sepsis treatment and, thereby, improvement in outcomes. Ideally, future studies will examine muscle tissue as well as blood in order to confirm the relevance of plasma changes.

With any biomarker panel there remains the possibility of over-fitting. However, in the present study, reproducibility in internal and external validation sets, replication with targeted assays and SVM analysis suggest that the sparse (seven-feature) panel has validity for prediction of sepsis-related mortality when applied at patient presentation in an emergency department setting. This study has limitations. The biological sample chosen for analysis was peripheral blood. As such, we cannot draw conclusions about the effects of sepsis on other target tissues. Furthermore, blood samples were analyzed at only two time points. Additional collections would have allowed a temporal analysis of sepsis changes that, giving a more precise view of changes through sepsis convalescence or deterioration. The number of non-survivors tested was relatively small, and confirmatory studies are needed. The number of non-sepsis deaths was small. As a result, we do not know if the outcome predictive signature is specific for sepsis or may also differentiate other acutely ill patient groups.

Finally, global and temporal correlations of metabolome and proteome data from relevant biological fluids in well-phenotyped patient groups appears suitable for expanding our understanding of intermediary metabolism, particularly with respect to poorly annotated analytes, and for characterization of homogeneous subgroups in complex traits. Combinations of transcriptome, proteome, metabolome, and genetic data may establish multi-dimensional molecular models of complex diseases that can provide insights into network responses to perturbation.

MATERIALS AND METHODS

Study Design

Pre-defined study components—Metabolomic and proteomic analysis was predicted to require 30 samples per group (non-infected controls, uncomplicated sepsis, severe sepsis, septic shock, and sepsis nonsurvivors) for 80% power to detect differences. Enrollment was performed during daytime hours through a convenience sampling and continued until this goal was met. Inclusion criteria included adults in the emergency department with known or suspected acute infection and the presence of at least two SIRS criteria. Exclusions were as previously described (12, 17, 25). Outliers were identified using various techniques including overlaid kernel density estimates, univariate distribution results, Mahalanobis Distances, and correlation coefficients.

Rationale and Design—Sepsis is a leading cause of death in the United States and there remain few therapeutic options. Understanding the pathobiology of sepsis outcomes can enable personalized patient management protocols and improve survival. In this study, clinical care was not standardized but rather was determined by individual providers. We collected clinical data including infection likelihood, infection type, microbiological etiologies, sepsis severity, and 28-day mortality. Serum of enrolled patients was taken at presentation and 24h later. Metabolomics and proteomics were performed using mass-spectroscopy techniques. Comprehensive, integrated analysis of serum metabolome and proteome data was performed to prioritize sepsis outcome signals. Logistic regression and support vector machine analysis was performed to predict patient outcomes.

Randomization—Patients were assigned to pre-defined clinical groups (non-infected controls, uncomplicated sepsis, severe sepsis, septic shock, and sepsis nonsurvivors) after retrospective clinical adjudications were performed. These assignments were made solely on the basis of information available in the medical record and were blind to any metabolomic or proteomic data, which had not yet been generated. Patients were matched for age, race, sex, and enrollment site using the sepsis nonsurvivor group as the reference.

Replication—The clinical, metabolomic and proteomic analyses were replicated in a separate CAPSOD subset of 18 sepsis nonsurvivors and 34 matched sepsis survivors (at t_0 [Vt_0] and t_{24} [Vt_{24}]). A second validation set was performed in an independent sepsis study (the Brigham and Women's Hospital Registry of Critical Illness cohort [RoCI], approved by the Partners Human Research Committee, protocol # 2008-P-000495) (27). This validation cohort had 29 non-infected patients with SIRS, 36 sepsis survivors and 25 sepsis nonsurvivors. The study followed the Equator Network Library recommendation for biospecimens and conforms to BRISQ Tier 1 reporting (77). Details are provided throughout the text. In addition, samples were stabilized in standard serum collection tubes. They were frozen for long-term preservation and then stored at −80°C until testing occurred, which was within one to five years. When necessary, samples were shipped on dry ice.

Patient Enrollment

Patients presenting at EDs (Henry Ford Hospital, Duke University Hospital, and Durham Veterans Affairs Medical Center) with suspected sepsis (≥2 SIRS criteria and infection) were enrolled (12, 25). Approval was obtained by institutional ethics committees and filed at (ClinicalTrials.gov (NCT00258869). Written informed consent was given by each patient or legal designate. Physical examination was performed and venous plasma and whole blood was collected at enrollment (t_0) and 24 hrs later (t_{24}); patients were followed for 28 days. Demographic and clinical data was anonymized and stored in compliance with HIPAA regulations (ProSanos Inc.). Following independent audit of infection status and outcomes, 150 subjects were chosen for derivation studies. Patients were classified as non-infected SIRS, uncomplicated sepsis, severe sepsis, septic shock, or sepsis nonsurvivor. Fifty-two sepsis survivors and deaths at t_0 and t_{24} samples were also utilized as an internal validation set. Recruitment for the BWH Registry of Critical Illness (RoCI) has been described in detail elsewhere (27). Briefly, demographic, clinical information, and blood specimens were collected from patients with critical illness in the medical intensive care unit (MICU) of the Brigham and Women's Hospital (BWH). Blood specimens were obtained within 2 days of ICU admission (Day 1), and also at days 3 and 7. Informed consent was obtained directly from patients, or, if not possible, their legal representatives. 400 subjects have been enrolled in RoCI from 2008 to 2012. Serum samples from 90 subjects on Day 1 of enrollment were selected for metabolomic profiling. RoCI is approved by the Partners Human Research Committee under IRB protocol 2008-P-000495.

Semi-quantitative metabolomic analysis

Non-targeted UPLC-MS/MS and GC-MS analyses were performed at Metabolon, Inc. as described (78–80). The UPLC-MS/MS platform utilized a Waters Acquity UPLC with Waters UPLC BEH C18-2.1×100 mm, 1.7 μm columns and a ThermoFisher LTQ mass spectrometer. GC-MS was performed on a Thermo-Finnigan Trace DSQ fast-scanning single-quadrupole MS. Metabolites were identified by automated comparison of the ion features in the experimental samples to a reference library of chemical standard entries that included retention time, molecular weight (m/z), preferred adducts, and in-source fragments as well as associated MS spectra and curated by visual inspection for quality control using software developed at Metabolon (81). Peaks were quantified using area-under-the-curve. Raw area counts for each metabolite in each sample were normalized to correct for variation resulting from instrument inter-day tuning differences by the median value for each run-day, therefore, setting the medians to 1.0 for each run. Missing values were imputed with the observed minimum after normalization. However, metabolites with missing values in >50% of the samples were excluded from analysis.

Quantitative metabolomics analysis

50μL of 382 human EDTA plasma samples, 48 quality control plasma aliquots, 6 calibration standards and a blank internal standard (H_2O) were treated (see supplemental materials and methods) and injected onto a Waters Acquity UPLC/Thermo Quantum Ultra triple quadrupole LC/MS/MS with HESI source equipped with a reversed phase chromatographic column system to determine quantitative changes for methylbutyroylcarnitine, 4-cis-decenoylcarnitine, butyroylcarnitine, hexanoylcarnitine, 4-methyl-2-oxopentanoate, 1-arachidonoylglycerophosphocholine, 1-linoleoylglycerophosphocholine, HPLA, 3-methoxytyrosine, n-acetylthreonine, and pseudouridine. The peak areas of the respective product ions were measured against the peak areas of the corresponding internal standard product ions (Fig. S9). Analyte concentrations are reported in the weight/volume format ("ug/mL") and not in molar concentrations; Quantitation was performed using weighted linear least squares regression analysis generated from fortified calibration standards prepared immediately prior to each run (Fig. S10). Correlation analysis of quantitative results to semi-quantitative analysis was high (Fig. S11).

Proteomic analysis

Plasma proteomic analysis was performed by Monarch Life Sciences Inc. as previously described (82). Briefly, tryptic digests (~20 μg) with the most abundant proteins removed (see supplemental materials and methods) were analyzed using a Thermo-Fisher Scientific LTQ linear ion-trap mass spectrometer coupled with a Surveyor HPLC system. Data were collected and analyzed as described (83, 84). Database searches against the IPI (International Protein Index) human database (v3.48) and the non-Redundant-*Homo Sapiens* database (update July 2009) were carried out using both the X!Tandem and SEQUEST algorithms (85, 86). The q-value represented peptide false identification rate and was calculated by incorporating Sequest and X!Tandem results (83). Observed peptide MS/MS spectrum and theoretically derived spectra were used to assign quality scores (Xcorr in SEQUEST and e-Score in X!Tandem). Peptides with high confidence (>90%) and multiple unique sequences were employed for analyses. Protein quantification was carried out using as described.(84). Area-under-the-curve (AUC) for each individually aligned peak from each sample was measured and compared for relative abundance and were log2 transformed before quantile normalization (87). Raw LC-MS/MS data files were independently validated by the Duke Proteomics Core using spectral counting in the form of number of identified spectra per protein (see supplemental materials and methods).

Statistical analysis

Overlaid kernel density estimates, univariate distribution results, Mahalanobis Distances, correlation coefficients of pair wise sample comparisons, unsupervised principal components analysis (by Pearson product-moment correlation) and Ward hierarchal clustering of Pearson product-moment correlations were performed using $\log_2$-transformed data as described (88) with JMP Genomics 5.0 (SAS Institute). Decomposition of principal components of variance, including patient demographics, past medical history, laboratory and clinical values, was performed to maximize sepsis-group-related components of variance and minimize residual variance (88). Guided by these analyses, ANOVA was performed between sepsis groups, with 5 – 25% false discovery rate (FDR) correction (as noted in the text) and inclusion of substantive non-hypothesis components of variance as fixed effects (88). These included renal function, as determined by eGFR, hemodialysis (HD), cirrhosis and liver disease, hepatitis, neoplastic disease, and administration of exogenous immunosuppressants. Predictive modeling was performed with JMP Genomics 5.0 using logistic regression. Data is presented as average ± standard error of the mean (SEM). Bayesian clinical factor analysis [$c_j = By_j + A(s_j \circ z_j) + \varepsilon_j$] was performed to

distinguish the effects of clinical outcomes (uninfected SIRS group, sepsis survivors, and sepsis nonsurvivors) and relevant clinical factors on the metabolome (see supplemental materials). The significant features were then plotted on B-matrix as well as plotted as normalized energy (referred to as factor scores within the manuscript) of each clinical feature. Pairwise cross correlations were performed using JMP Genomics 5.0 software to compare protein and metabolite values at t_0 and t_{24} using Pearson moment-correlation. Protein-metabolite correlations were considered significant if observed at t_0 and t_{24} with p-values <0.05 and <0.1, or at a single time point with Bonferroni correction. Support vector machines (SVM), both linear and with RBF kernels, were used for binary classification of sepsis survivors and deaths. Performance was evaluated by test data scores for AUC and accuracy.

Supplementary Material

Refer to Web version on PubMed Central for supplementary material.

Acknowledgments

We thank Tom Gagliano for graphic arts, John Michael Langley for motivation and we thank the study subjects. *A Deo mirificatio, ab amicis auxilium* - To God for creativity, to friends for help.

Funding: Supported by grants from NIH (U01AI066569, P20RR016480, HHSN266200400064C), Pfizer Inc. and Roche Diagnostics Inc. The RoCI cohort was supported by grants from NIH (HL112747 and HL05530). ELT was supported by a National Research Service Award training grant provided by the Agency for Healthcare Research and Quality as well as a VA Career Development Award.

References

1. Angus DC, et al. Epidemiology of severe sepsis in the United States: analysis of incidence, outcome, and associated costs of care. Critical care medicine. 2001; 29:1303–1310. [PubMed: 11445675]
2. McCaig LF, Nawar EW. National Hospital Ambulatory Medical Care Survey: 2004 emergency department summary. Adv Data. 2006:1–29.
3. Kumar A, et al. Initiation of inappropriate antimicrobial therapy results in a fivefold reduction of survival in human septic shock. Chest. 2009; 136:1237–1248. [PubMed: 19696123]
4. Kollef MH, Sherman G, Ward S, Fraser VJ. Inadequate antimicrobial treatment of infections: a risk factor for hospital mortality among critically ill patients. Chest. 1999; 115:462–474. [PubMed: 10027448]
5. Gross PA. Hypotension and mortality in septic shock: the “golden hour”. Critical care medicine. 2006; 34:1819–1820. [PubMed: 16714981]
6. Rivers EP, Coba V, Visbal A, Whitmill M, Amponsah D. Management of sepsis: early resuscitation. Clinics in chest medicine. 2008; 29:689–704. [PubMed: 18954703]
7. Dellinger RP, et al. Surviving Sepsis Campaign: international guidelines for management of severe sepsis and septic shock: 2008. Critical care medicine. 2008; 36:296–327. [PubMed: 18158437]
8. Puskarich MA, et al. Outcomes of patients undergoing early sepsis resuscitation for cryptic shock compared with overt shock. Resuscitation. 2011; 82:1289–1293. [PubMed: 21752522]
9. Lundberg JS, et al. Septic shock: an analysis of outcomes for patients with onset on hospital wards versus intensive care units. Critical care medicine. 1998; 26:1020–1024. [PubMed: 9635649]
10. Rivers E, et al. Early goal-directed therapy in the treatment of severe sepsis and septic shock. N Engl J Med. 2001; 345:1368–1377. [PubMed: 11794169]
11. Knaus WA, Draper EA, Wagner DP, Zimmerman JE. APACHE II: a severity of disease classification system. Critical care medicine. 1985; 13:818–829. [PubMed: 3928249]
12. Glickman SW, et al. Disease progression in hemodynamically stable patients presenting to the emergency department with sepsis. Acad Emerg Med. 2010; 17:383–390. [PubMed: 20370777]

13. Annane D, Aegerter P, Jars-Guincestre MC, Guidet B, Network CUR. Current epidemiology of septic shock: the CUB-Rea Network. American journal of respiratory and critical care medicine. 2003; 168:165–172. [PubMed: 12851245]
14. Green JP, Berger T, Garg N, Shapiro NI. Serum lactate is a better predictor of short-term mortality when stratified by C-reactive protein in adult emergency department patients hospitalized for a suspected infection. Annals of emergency medicine. 2011; 57:291–295. [PubMed: 21111512]
15. Jaimes F, et al. The systemic inflammatory response syndrome (SIRS) to identify infected patients in the emergency room. Intensive care medicine. 2003; 29:1368–1371. [PubMed: 12830377]
16. Vincent JL, et al. Use of the SOFA score to assess the incidence of organ dysfunction/failure in intensive care units: results of a multicenter, prospective study. Working group on "sepsis-related problems" of the European Society of Intensive Care Medicine. Crit Care Med. 1998; 26:1793–1800. [PubMed: 9824069]
17. Tsalik EL, et al. Discriminative value of inflammatory biomarkers for suspected sepsis. The Journal of emergency medicine. 2012; 43:97–106. [PubMed: 22056545]
18. Kingsmore, SF.; Lejnine, SJ.; Driscoll, M.; Tchernev, VT. United States Patent. 8,029,982. 2011.
19. LaRosa SP, Opal SM. Biomarkers: the future. Critical care clinics. 2011; 27:407–419. [PubMed: 21440209]
20. Pierrakos C, Vincent JL. Sepsis biomarkers: A review. Crit Care. 2010; 14:R15. [PubMed: 20144219]
21. Wheeler AP. Recent developments in the diagnosis and management of severe sepsis. Chest. 2007; 132:1967–1976. [PubMed: 18079230]
22. Noritomi DT, et al. Metabolic acidosis in patients with severe sepsis and septic shock: a longitudinal quantitative study. Crit Care Med. 2009; 37:2733–2739. [PubMed: 19885998]
23. Hotchkiss RS, Karl IE. The pathophysiology and treatment of sepsis. N Engl J Med. 2003; 348:138–150. [PubMed: 12519925]
24. Sauer U, Heinemann M, Zamboni N. Genetics. Getting closer to the whole picture. Science. 2007; 316:550–551. [PubMed: 17463274]
25. Tsalik EL, et al. Multiplex PCR to diagnose bloodstream infections in patients admitted from the emergency department with sepsis. Journal of clinical microbiology. 2010; 48:26–33. [PubMed: 19846634]
26. Bernard GR, et al. Efficacy and safety of recombinant human activated protein C for severe sepsis. N Engl J Med. 2001; 344:699–709. [PubMed: 11236773]
27. Dolinay T, et al. Inflammasome-regulated cytokines are critical mediators of acute lung injury. American journal of respiratory and critical care medicine. 2012; 185:1225–1234. [PubMed: 22461369]
28. Sreekumar A, et al. Metabolomic profiles delineate potential role for sarcosine in prostate cancer progression. Nature. 2009; 457:910–914. [PubMed: 19212411]
29. Wishart DS, et al. HMDB: a knowledgebase for the human metabolome. Nucleic acids research. 2009; 37:D603–610. [PubMed: 18953024]
30. Marshall JC. Such stuff as dreams are made on: mediator-directed therapy in sepsis. Nat Rev Drug Discov. 2003; 2:391–405. [PubMed: 12750742]
31. Lissauer E, Johnson B, Shi S, Gentle T, Scalea M. 128 Decreased lysophosphatidylcholine levels are associated with sepsis compared to uninfected inflammation prior to onset of sepsis. Journal of Surgical Research. 2007; 137:206–206.
32. Drobnik W, et al. Plasma ceramide and lysophosphatidylcholine inversely correlate with mortality in sepsis patients. Journal of lipid research. 2003; 44:754–761. [PubMed: 12562829]
33. Tabb DL, et al. Repeatability and reproducibility in proteomic identifications by liquid chromatography-tandem mass spectrometry. J Proteome Res. 2010; 9:761–776. [PubMed: 19921851]
34. Qian WJ, Jacobs JM, Liu T, Camp DG 2nd, Smith RD. Advances and challenges in liquid chromatography-mass spectrometry-based proteomics profiling for clinical applications. Molecular & cellular proteomics: MCP. 2006; 5:1727–1744. [PubMed: 16887931]

35. Edgar JD, Gabriel V, Gallimore JR, McMillan SA, Grant J. A prospective study of the sensitivity, specificity and diagnostic performance of soluble intercellular adhesion molecule 1, highly sensitive C-reactive protein, soluble E-selectin and serum amyloid A in the diagnosis of neonatal infection. BMC Pediatr. 2010; 10:22. [PubMed: 20398379]
36. Ng PC, et al. Host-response biomarkers for diagnosis of late-onset septicemia and necrotizing enterocolitis in preterm infants. J Clin Invest. 2010; 120:2989–3000. [PubMed: 20592468]
37. Buller HR, et al. Postoperative hemostatic profile in relation to gram-negative septicemia. Crit Care Med. 1982; 10:311–315. [PubMed: 7075222]
38. Helling H, et al. Fibrinolytic and procoagulant activity in septic and haemorrhagic shock. Clin Hemorheol Microcirc. 2010; 45:295–300. [PubMed: 20675912]
39. Iossa S, et al. Acetyl-L-carnitine supplementation differently influences nutrient partitioning, serum leptin concentration and skeletal muscle mitochondrial respiration in young and old rats. J Nutr. 2002; 132:636–642. [PubMed: 11925454]
40. Cortes CVV. Support Vector Networks. Machine Learning. 1995; 20:273–297.
41. Kingsmore SF, et al. Identification of diagnostic biomarkers for infection in premature neonates. Molecular & cellular proteomics: MCP. 2008; 7:1863–1875. [PubMed: 18622029]
42. Bone RC, et al. Definitions for sepsis and organ failure and guidelines for the use of innovative therapies in sepsis. The ACCP/SCCM Consensus Conference Committee. American College of Chest Physicians/Society of Critical Care Medicine. Chest. 1992; 101:1644–1655. [PubMed: 1303622]
43. Feingold KR, Wang Y, Moser A, Shigenaga JK, Grunfeld C. LPS decreases fatty acid oxidation and nuclear hormone receptors in the kidney. J Lipid Res. 2008; 49:2179–2187. [PubMed: 18574256]
44. Houten SM, Wanders RJ. A general introduction to the biochemistry of mitochondrial fatty acid beta-oxidation. Journal of inherited metabolic disease. 2010; 33:469–477. [PubMed: 20195903]
45. Wu Y, Song Y, Belardinelli L, Shryock JC. The late Na+ current (INa) inhibitor ranolazine attenuates effects of palmitoyl-L-carnitine to increase late INa and cause ventricular diastolic dysfunction. J Pharmacol Exp Ther. 2009; 330:550–557. [PubMed: 19403851]
46. Lang TF. Adult presentations of medium-chain acyl-CoA dehydrogenase deficiency (MCADD). J Inherit Metab Dis. 2009; 32:675–683. [PubMed: 19821147]
47. Feingold K, Kim MS, Shigenaga J, Moser A, Grunfeld C. Altered expression of nuclear hormone receptors and coactivators in mouse heart during the acute-phase response. American journal of physiology Endocrinology and metabolism. 2004; 286:E201–207. [PubMed: 14701665]
48. Feingold KR, Moser A, Patzek SM, Shigenaga JK, Grunfeld C. Infection decreases fatty acid oxidation and nuclear hormone receptors in the diaphragm. Journal of lipid research. 2009; 50:2055–2063. [PubMed: 19443862]
49. Kim MS, Shigenaga JK, Moser AH, Feingold KR, Grunfeld C. Suppression of estrogen-related receptor alpha and medium-chain acyl-coenzyme A dehydrogenase in the acute-phase response. Journal of lipid research. 2005; 46:2282–2288. [PubMed: 16061943]
50. Zingarelli B, et al. Peroxisome proliferator-activated receptor {delta} regulates inflammation via NF-{kappa}B signaling in polymicrobial sepsis. The American journal of pathology. 2010; 177:1834–1847. [PubMed: 20709805]
51. Kapoor A, et al. Protective role of peroxisome proliferator-activated receptor-beta/delta in septic shock. American journal of respiratory and critical care medicine. 2010; 182:1506–1515. [PubMed: 20693380]
52. Djouadi F, Bastin J. PPARalpha gene expression in the developing rat kidney: role of glucocorticoids. Journal of the American Society of Nephrology: JASN. 2001; 12:1197–1203. [PubMed: 11373342]
53. Mandard S, Muller M, Kersten S. Peroxisome proliferator-activated receptor alpha target genes. Cellular and molecular life sciences: CMLS. 2004; 61:393–416. [PubMed: 14999402]
54. Standage SW, Caldwell CC, Zingarelli B, Wong HR. Reduced peroxisome proliferator-activated receptor alpha expression is associated with decreased survival and increased tissue bacterial load in sepsis. Shock. 2012; 37:164–169. [PubMed: 22089192]

55. Valkner K, Ely S, Kerner J, Scott J, Bieber LL. Effect of hypoxia on pig heart short-chain acylcarnitines. Comparative biochemistry and physiology A, Comparative physiology. 1985; 80:123–127.
56. Yan JJ, et al. Therapeutic effects of lysophosphatidylcholine in experimental sepsis. Nature medicine. 2004; 10:161–167.
57. Rice TW, et al. Enteral omega-3 fatty acid, gamma-linolenic acid, and antioxidant supplementation in acute lung injury. JAMA: the journal of the American Medical Association. 2011; 306:1574–1581. [PubMed: 21976613]
58. Brealey D, et al. Association between mitochondrial dysfunction and severity and outcome of septic shock. Lancet. 2002; 360:219–223. [PubMed: 12133657]
59. Carre JE, et al. Survival in critical illness is associated with early activation of mitochondrial biogenesis. Am J Respir Crit Care Med. 2010; 182:745–751. [PubMed: 20538956]
60. Fredriksson K, et al. Dysregulation of mitochondrial dynamics and the muscle transcriptome in ICU patients suffering from sepsis induced multiple organ failure. PloS one. 2008; 3:e3686. [PubMed: 18997871]
61. Gellerich FN, et al. Impaired energy metabolism in hearts of septic baboons: diminished activities of Complex I and Complex II of the mitochondrial respiratory chain. Shock. 1999; 11:336–341. [PubMed: 10353539]
62. Giovannini I, et al. Respiratory quotient and patterns of substrate utilization in human sepsis and trauma. JPEN J Parenter Enteral Nutr. 1983; 7:226–230. [PubMed: 6408272]
63. Kreymann G, et al. Oxygen consumption and resting metabolic rate in sepsis, sepsis syndrome, and septic shock. Critical care medicine. 1993; 21:1012–1019. [PubMed: 8319458]
64. Long CL. Energy balance and carbohydrate metabolism in infection and sepsis. Am J Clin Nutr. 1977; 30:1301–1310. [PubMed: 888781]
65. Pyle A, et al. Fall in circulating mononuclear cell mitochondrial DNA content in human sepsis. Intensive Care Med. 36:956–962. [PubMed: 20224905]
66. Zhang Q, et al. Circulating mitochondrial DAMPs cause inflammatory responses to injury. Nature. 2010; 464:104–107. [PubMed: 20203610]
67. Tannahill GM, et al. Succinate is an inflammatory signal that induces IL-1beta through HIF-1alpha. Nature. 2013; 496:238–242. [PubMed: 23535595]
68. Brealey D, et al. Mitochondrial dysfunction in a long-term rodent model of sepsis and organ failure. Am J Physiol Regul Integr Comp Physiol. 2004; 286:R491–497. [PubMed: 14604843]
69. Haden DW, et al. Mitochondrial biogenesis restores oxidative metabolism during Staphylococcus aureus sepsis. Am J Respir Crit Care Med. 2007; 176:768–777. [PubMed: 17600279]
70. Piantadosi CA. Regulation of mitochondrial processes by protein S-nitrosylation. Biochim Biophys Acta. 2011
71. Singer M, De Santis V, Vitale D, Jeffcoate W. Multiorgan failure is an adaptive, endocrine-mediated, metabolic response to overwhelming systemic inflammation. Lancet. 2004; 364:545–548. [PubMed: 15302200]
72. Suliman HB, et al. Toll-like receptor 4 mediates mitochondrial DNA damage and biogenic responses after heat-inactivated E. coli. FASEB J. 2005; 19:1531–1533. [PubMed: 15994412]
73. Scarpulla RC, Vega RB, Kelly DP. Transcriptional integration of mitochondrial biogenesis. Trends in endocrinology and metabolism: TEM. 2012; 23:459–466. [PubMed: 22817841]
74. Hotchkiss RS, et al. Apoptotic cell death in patients with sepsis, shock, and multiple organ dysfunction. Crit Care Med. 1999; 27:1230–1251. [PubMed: 10446814]
75. Calvano SE, et al. A network-based analysis of systemic inflammation in humans. Nature. 2005; 437:1032–1037. [PubMed: 16136080]
76. Zhou B, et al. Analysis of factorial time-course microarrays with application to a clinical study of burn injury. Proc Natl Acad Sci U S A. 2010; 107:9923–9928. [PubMed: 20479259]
77. Moore HM, et al. Biospecimen reporting for improved study quality (BRISQ). Cancer cytopathology. 2011; 119:92–101. [PubMed: 21433001]
78. Evans AM, DeHaven CD, Barrett T, Mitchell M, Milgram E. Integrated, nontargeted ultrahigh performance liquid chromatography/electrospray ionization tandem mass spectrometry platform

for the identification and relative quantification of the small-molecule complement of biological systems. Anal Chem. 2009; 81:6656–6667. [PubMed: 19624122]

79. Weiner J 3rd, et al. Biomarkers of inflammation, immunosuppression and stress with active disease are revealed by metabolomic profiling of tuberculosis patients. PloS one. 2012; 7:e40221. [PubMed: 22844400]
80. Sha W, et al. Metabolomic profiling can predict which humans will develop liver dysfunction when deprived of dietary choline. FASEB journal: official publication of the Federation of American Societies for Experimental Biology. 2010; 24:2962–2975. [PubMed: 20371621]
81. Dehaven CD, Evans AM, Dai H, Lawton KA. Organization of GC/MS and LC/MS metabolomics data into chemical libraries. Journal of cheminformatics. 2010; 2:9. [PubMed: 20955607]
82. Hale JE, Butler JP, Gelfanova V, You JS, Knierman MD. A simplified procedure for the reduction and alkylation of cysteine residues in proteins prior to proteolytic digestion and mass spectral analysis. Anal Biochem. 2004; 333:174–181. [PubMed: 15351294]
83. Higgs RE, et al. Estimating the statistical significance of peptide identifications from shotgun proteomics experiments. J Proteome Res. 2007; 6:1758–1767. [PubMed: 17397207]
84. Higgs RE, Knierman MD, Gelfanova V, Butler JP, Hale JE. Comprehensive label-free method for the relative quantification of proteins from biological samples. J Proteome Res. 2005; 4:1442–1450. [PubMed: 16083298]
85. Craig R, Beavis RC. TANDEM: matching proteins with tandem mass spectra. Bioinformatics. 2004; 20:1466–1467. [PubMed: 14976030]
86. Yates JR 3rd, Eng JK, McCormack AL, Schieltz D. Method to correlate tandem mass spectra of modified peptides to amino acid sequences in the protein database. Anal Chem. 1995; 67:1426–1436. [PubMed: 7741214]
87. Bolstad BM, Irizarry RA, Astrand M, Speed TP. A comparison of normalization methods for high density oligonucleotide array data based on variance and bias. Bioinformatics. 2003; 19:185–193. [PubMed: 12538238]
88. Mudge J, et al. Genomic convergence analysis of schizophrenia: mRNA sequencing reveals altered synaptic vesicular transport in post-mortem cerebellum. PloS one. 2008; 3:e3625. [PubMed: 18985160]
89. Vincent JL, et al. The SOFA (Sepsis-related Organ Failure Assessment) score to describe organ dysfunction/failure. On behalf of the Working Group on Sepsis-Related Problems of the European Society of Intensive Care Medicine. Intensive care medicine. 1996; 22:707–710. [PubMed: 8844239]
90. Balk RA. Severe sepsis and septic shock. Definitions, epidemiology, and clinical manifestations. Critical care clinics. 2000; 16:179–192. [PubMed: 10768078]
91. Poggio ED, Wang X, Greene T, Van Lente F, Hall PM. Performance of the modification of diet in renal disease and Cockcroft-Gault equations in the estimation of GFR in health and in chronic kidney disease. J Am Soc Nephrol. 2005; 16:459–466. [PubMed: 15615823]
92. Lawton KA, et al. Analysis of the adult human plasma metabolome. Pharmacogenomics. 2008; 9:383–397. [PubMed: 18384253]
93. Keller A, Nesvizhskii AI, Kolker E, Aebersold R. Empirical statistical model to estimate the accuracy of peptide identifications made by MS/MS and database search. Anal Chem. 2002; 74:5383–5392. [PubMed: 12403597]
94. Nesvizhskii AI, Keller A, Kolker E, Aebersold R. A statistical model for identifying proteins by tandem mass spectrometry. Anal Chem. 2003; 75:4646–4658. [PubMed: 14632076]

Editor's Summary

Heading: Understanding survival of the fittest in sepsis

Differentiating mild infections from life-threatening ones is a complex decision that is made millions of times a year in US emergency rooms. Should a patient be sent home with antibiotics and chicken soup? Or should he or she be hospitalized for intensive treatment? Sepsis – infection that is associated with a generalized inflammatory response – is one of the leading causes of death. In two prospective clinical studies, patients arriving at four urban emergency departments with symptoms of sepsis were evaluated clinically and by analysis of their plasma proteome and metabolome. Survivors and non-survivors at 28-days were compared and a molecular signature was detected that appeared to differentiate these outcomes – even as early as the time of hospital arrival. The signature was part of a large set of differences between these groups showing that better energy-producing fatty acid catabolism was associated with survival of the fittest in sepsis. A test developed from the signature was able to predict sepsis survival and nonsurvival reproducibly and better than current methods. This test could help to make that all important decision in the emergency room a more accurate one.

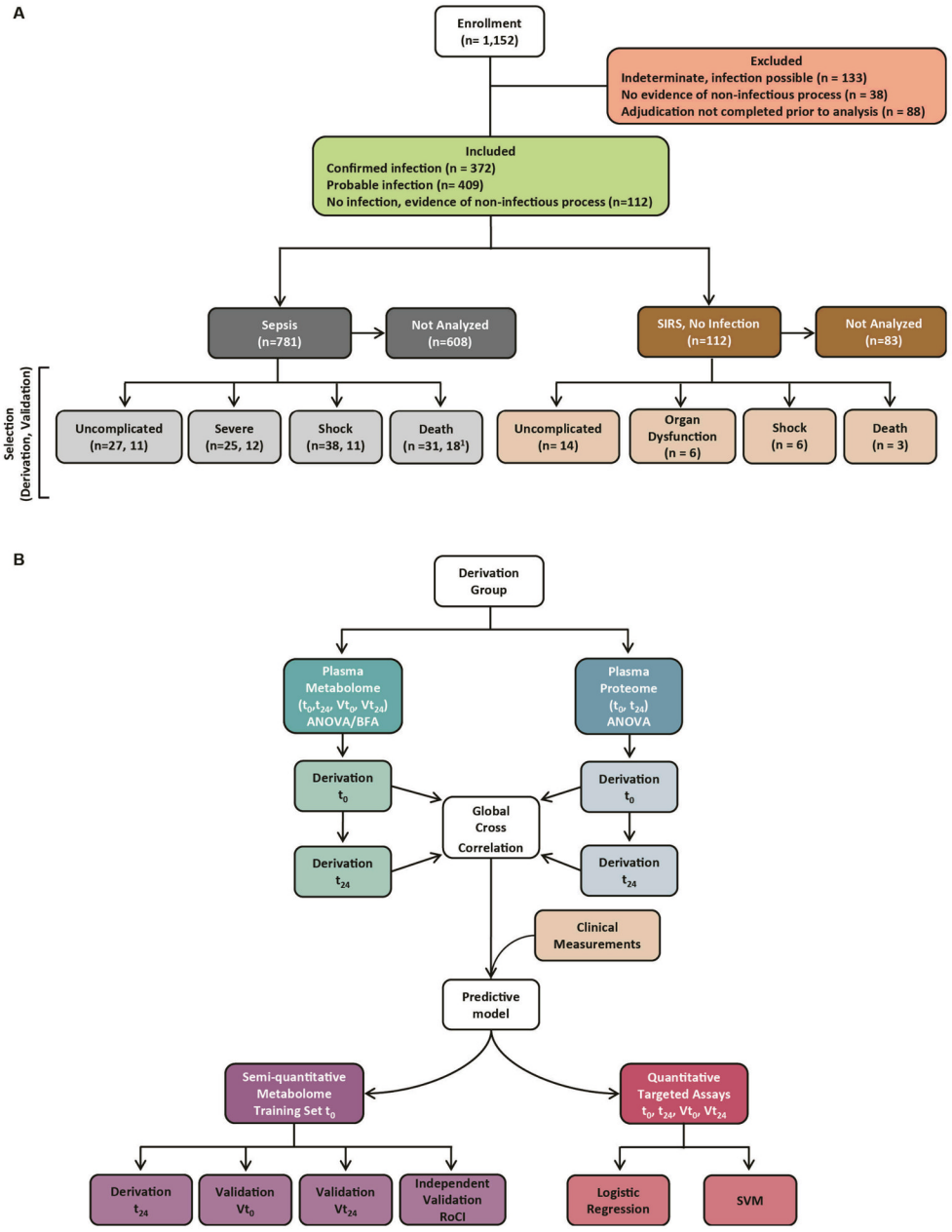

Figure 1. An integrative systems survey of sepsis survival and death

(A) CONSORT flow chart of patient enrollment and selection. Patients presenting to emergency departments with suspected community-acquired sepsis (acute infection and ≥2 SIRS criteria) were grouped according to final adjudication (sepsis or SIRS, no infection), day 3 clinical course (septic shock, severe sepsis, and uncomplicated sepsis) and outcome at day 28 (survival or death). Groups were defined by the most severe stage of sepsis attained. A subset of cases were chosen for the derivation study based upon planned number (n=30) of patients per subgroup and enriched for etiologic agents and controlling for attributes defined by the sepsis nonsurvivor group. The validation group had limited number of sepsis nonsurvivors. [1] One sepsis nonsurvivor initially refused phlebotomy at t_0, yet later agreed at t_{24}. The sample was utilized to maximize validation predictive modeling studies. No non-infected SIRS validation samples were selected because predictive modeling was not

successful during derivation. **(B)** Experimental design. MS-based metabolome and proteome analysis was performed on plasma samples obtained at t_0 and t_{24} from 150 matched derivation subjects. Validation of metabolome findings was sought by semi-quantitative MS in an independent cohort comprising all remaining sepsis nonsurvivors and a matched group of sepsis survivors at t_0 and t_{24} (n=52). Following molecular integration and analysis, predictive models were developed that were representative of the clinical and molecular findings. A top model utilizing semi-quantitative metabolomics clinical measures was trained at t_0, and then tested against the derivation t_{24} group, validation groups (Vt_0, Vt_{24}) and an independent validation (RoCI) cohort. The utility of the predictive models was further tested by clinical measures and targeted, quantitative assays of butyroylcarnitine, 2-methylbytyroylcarnitine, hexanoylcarnitine, cis-4-decenoylcarnitine, 1-arachidonoyl-glycerophosphocholine (GPC), 1-linoleoyl-GPC, pseudouridine, 3-(4-hydroxyphenyl)lactate (HPLA), 4-methyl-2-oxopentanoate, 3-methoxytyrosine and N-acetylthreonine of 382 samples, four samples were not included in a subset of metabolites due to limited serum volume. Tests included logistic regression of the top model derived by semi-quantitative results and Support Vector Machine (SVM) analysis of the top model.

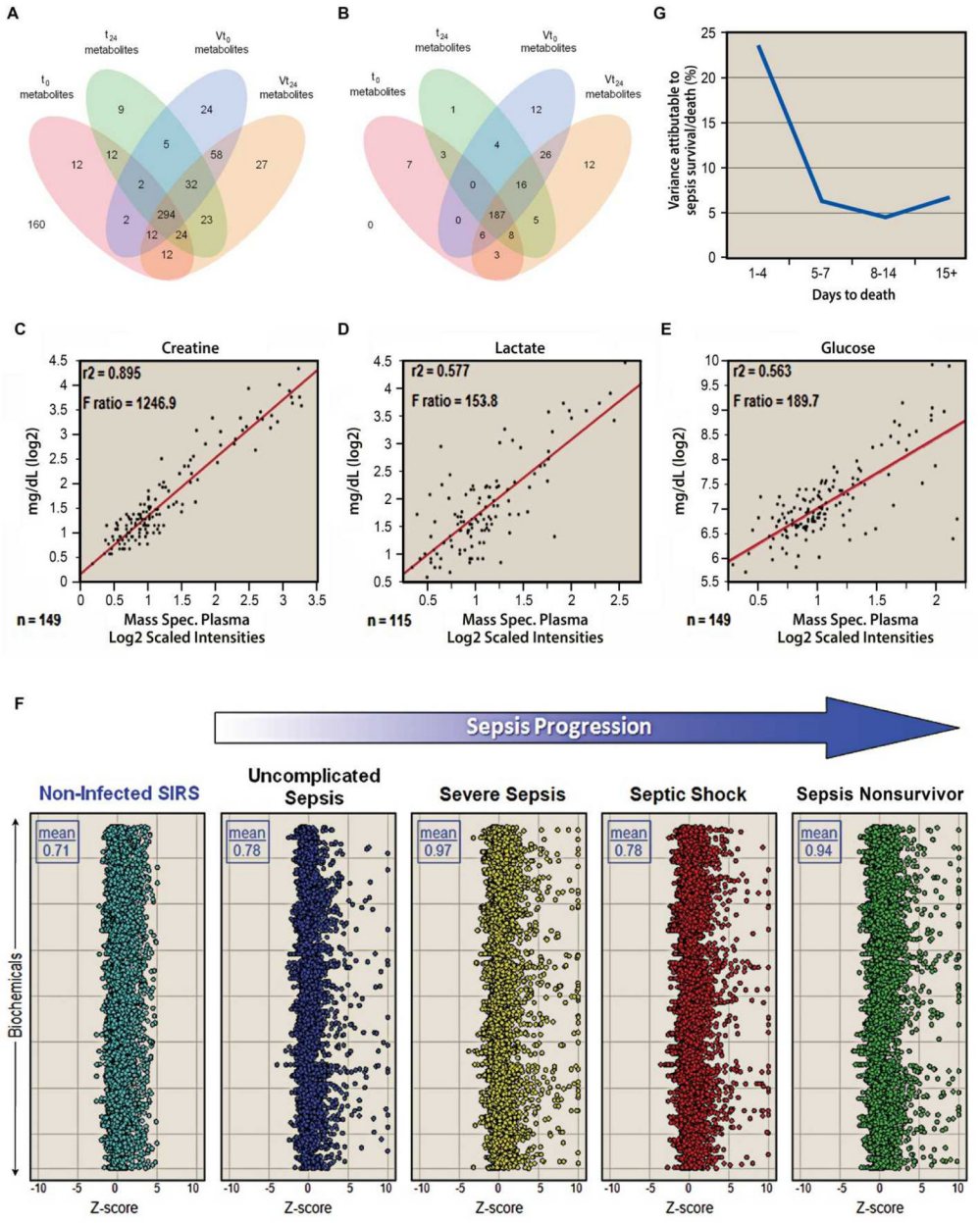

Figure 2. Metabolomic profiling of plasma in sepsis

(A, B) Venn diagrams of overlap of biochemicals (A) and annotated metabolites (B) measured by MS in discovery plasma samples at t_0 (n=150) and t_{24} (n=132) and 52 Validation (V) patients at t_0 and t_{24}. 160 metabolites were removed from the analysis because they were detected in ≥ 50% of the patients. (**C–E**) Comparison of Creatinine (C), Lactate (D) and Glucose (E) concentrations as determined in serum by clinical chemical analyzer and in plasma by MS in 149, 115 and 149 patients, respectively. Differences in n-values were due to omissions in clinical values – a large group of patients did not require blood lactate values as part of their clinical care. MS values are normalized, log-transformed intensities. Clinical chemistry values (mg/dl) are log-transformed. **(F)** Z-score scatter plots of plasma metabolites from non-infected SIRS, uncomplicated sepsis, severe sepsis, septic shock or sepsis nonsurvivor patients. Zero on the X-axis represents the mean of the control

group. Each data point is expressed as the number of standard deviations from the mean of the controls. The Y-axis shows all values for each biochemical on the same horizontal line. Z-score values are standard deviations from the control mean, revealing changes relative to control. The boxed values are *m*Scores, which are averages of the absolute values of Z-scores for all metabolites, calculated using non-truncated, non-imputed values. (**G)** The variance in plasma metabolite concentrations at the time of emergency department enrollment (t_0) that was attributable to sepsis outcome decreased with increasing days-to-death (X-axis).

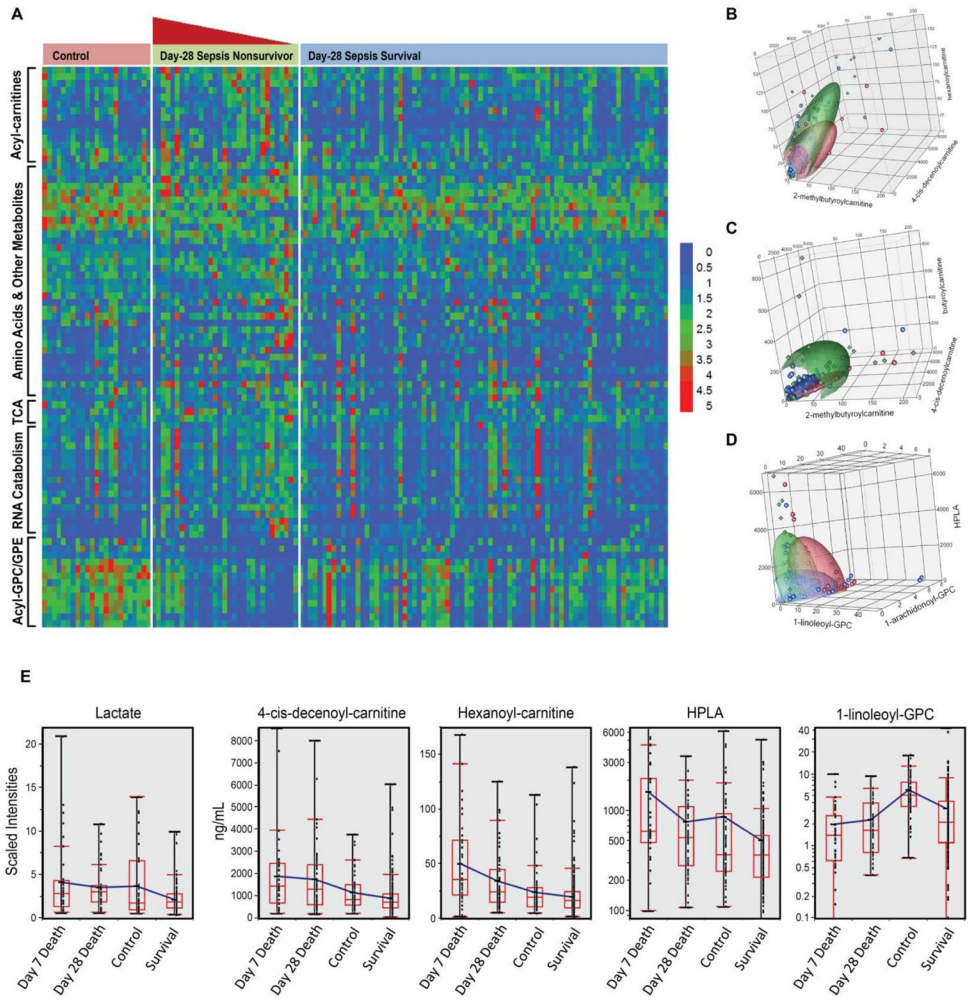

Figure 3. Comparisons of the plasma metabolome in community-acquired sepsis survivors and nonsurvivors

(A) Comparison of annotated plasma metabolite concentrations at t_{24} in 132 discovery subjects (represented by columns). Individuals who died were ordered by days-to-death (decreasing from left to right as indicated by the black triangle). Rows show 82 host metabolites with statistically significant differences between groups (stratified ANOVA, $p<0.05$). Colors indicate log-transformed standardized values. Highlighted are 13 acyl-glycerophosphocholines (GPCs) and acyl-glycerophosphoethanolamines (GPEs), which were decreased in sepsis survivors and further decreased in sepsis nonsurvivors (in comparison with controls), 13 RNA catabolites and 14 acyl-carnitines, both of which were decreased in sepsis survivors and increased in sepsis nonsurvivors (in comparison with controls). Detailed images in supplementary materials (Fig. S5). (**B–D**) Three-dimensional scatterplots showing plasma acyl-carnitine and acyl-GPC concentrations in 378 samples, as measured by quantitative, targeted assays. (**B, C**) Acylcarnitine concentrations were generally increased in day-28 sepsis nonsurvivors (green contour ellipsoid) and decreased in sepsis survivors (blue ellipsoid) when compared with non-infected controls (red ellipsoid). Samples obtained from patients who died with sepsis within the 28 day follow-up period are indicated by green diamonds (n=93; 4-cis-decenoylcarnitine 1825±168 mg/dL; hexanoylcarnitine 41.2±3.5 mg/dL; butyroylcarnitine 68.2±11.7 mg/dL [mean±S.E.M.]), sepsis survivors by blue dots (n=235; 4-cis-decenoylcarnitine 932±50 mg/dL;

hexanoylcarnitine 20.3±1.1 mg/dL; butyroylcarnitine 31.9±2.3 mg/dL) and non-infected controls by red dots (n=54; 4-cis-decenoylcarnitine 1200±115 mg/dL; hexanoylcarnitine 24.6±2.9 mg/dL; butyroylcarnitine 35.0±3.7 mg/dL). **(D)** Three -dimensional scatterplot showing similar trends in plasma values of two acyl-glycerophosphocholines (acyl-GPCs) and an RNA catabolite in 378 samples. Acyl-GPCs generally were highest in non-infected (red contour ellipsoid), lower in sepsis survivors (blue contour ellipsoid) and lowest in day-28 sepsis nonsurvivors (green contour ellipsoid). Sepsis day 28-deaths are shown by green diamonds (n=93; 1-arachidonoyl-GPC 1.10±0.09 mg/dL; 1-linoleoyl-GPC 2.23±0.21 mg/dL; pseudouridine 954±65 mg/dL [mean±S.E.M.]), sepsis survivors by blue dots (n=235; 1-arachidonoyl-GPC 1.38±0.07 mg/dL; 1-linoleoyl-GPC 3.40±0.29 mg/dL; pseudouridine 708±43 mg/dL) and non-infected controls by red dots (n=54; 1-arachidonoyl-GPC 2.49±0.13mg/dL; 1-linoleoyl-GPC 6.15±0.52 mg/dL; pseudouridine 628±88 mg/dL). Ellipsoids encompass 90% of sample values. **(E).** Box and whisker plots of MS lactate values and targeted, quantitative values (red boxes) in 378 plasma samples. Sample values are shown in black. Ranges are shown by black horizontal lines. Means are connected by blue lines.

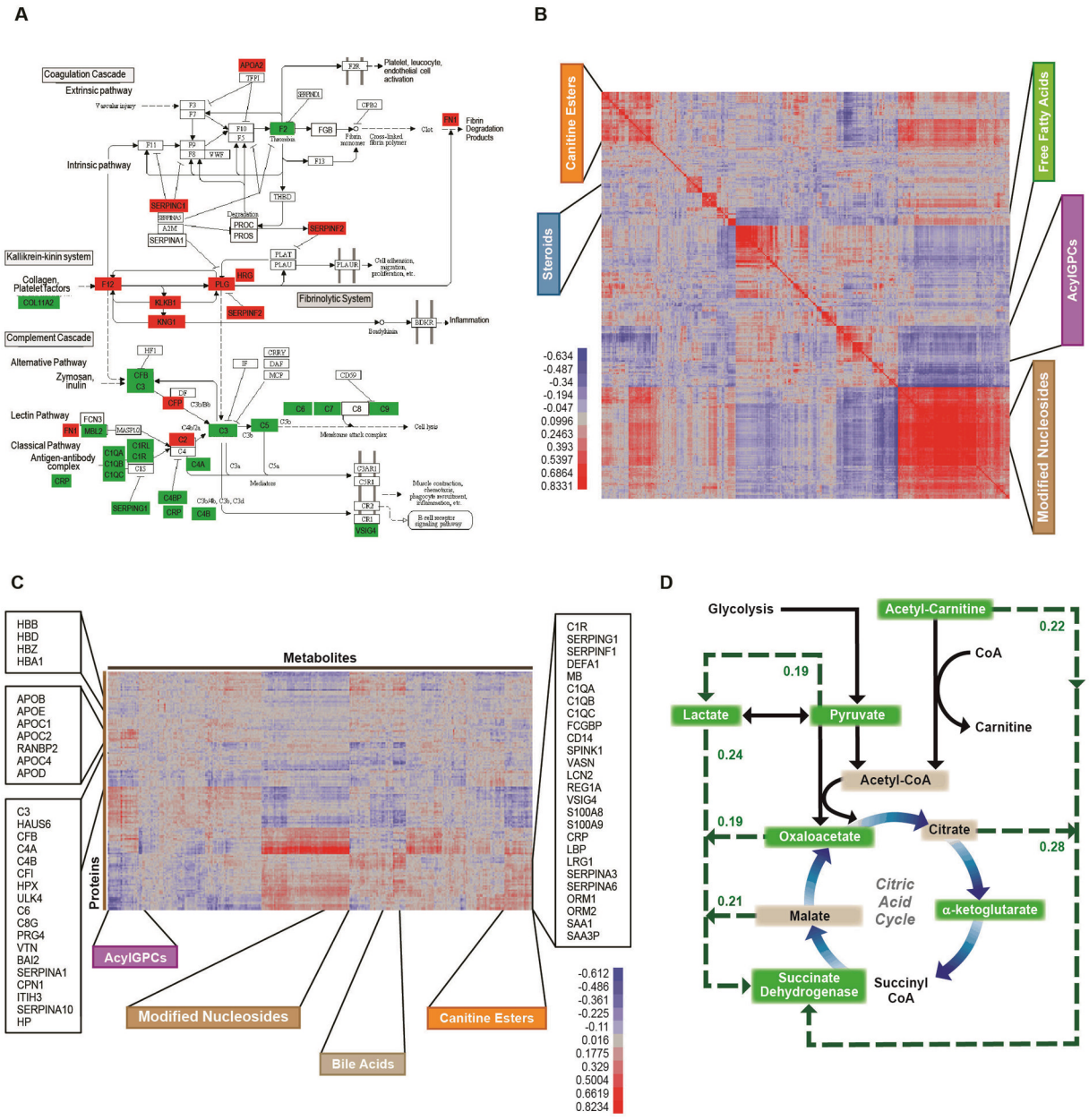

Figure 4. Integration of metabolomic and proteomic differences in sepsis nonsurvival

(A) Changes in plasma proteins in the complement, coagulation and fibrinolytic cascades in sepsis survivors and nonsurvivors. Adapted from KEGG. Red boxes indicate proteins that are decreased in sepsis nonsurvivors compared to survivors; Green boxes are increased in sepsis nonsurvivors. **(B)** Heatmap of hierarchical clustering of pairwise Pearson product-moment correlations of 332 log-transformed, annotated plasma metabolites in 132 subjects at t_0 compared to matched subjects at t_{24}. Positive correlations are red; inverse correlations are blue. Unannotated gas chromatography–mass spectrometry identified biochemicals were excluded from the analysis. A detailed list of the metabolite clusters are in the supplemental materials (Fig. S17). **(C)** Heatmap of hierarchical clustering of pairwise Pearson product-moment correlations of 162 log-transformed annotated plasma proteins and 332 metabolites in 132 subjects at t_0. 18 subjects at t_0 were not included within this analysis because there

was not a matched value at t_{24}. Positive correlations are red; inverse correlations are blue. Excluded were metabolites or proteins detected in <50% of patients or that did not have a reported value at both t_0 and t_{24}. **(D)** Plasma metabolite correlations with Succinate Dehydrogenase Complex, Subunit D (SDHD) was increased 2.44-fold in sepsis nonsurvival compared with sepsis survival. Regulation of metabolite flow from the pyruvate dehydrogenase complex through the citric acid cycle is shown, along with associated reactions that replenish depleted cycle intermediates and entry into fatty acid β-oxidation. Correlation coefficients of plasma metabolite with plasma SDHD values are indicated by green integers. Plasma lactate, pyruvate, acetyl-carnitine, oxaloacetate and α-ketoglutarate were higher in sepsis nonsurvivors than sepsis survivors. Global cross correlation analysis results determined from all relevant t_0 metabolites (336 biochemicals) correlated with t_0 proteins (165 proteins) in 150 derivation patient samples. The analysis included lower confidence protein acyl-coA synthetase M6 (ACSM6) and single time point high confidence proteins SDHD, and fatty acid binding protein 4.

Table 1

Clinical Variables and Demographics

	Derivation			Validation CAPSOD		RoCI		
Clinical Variable	**SIRS**	**Sepsis Survivors**	**Sepsis Nonsurvivors**	**Sepsis Survivors**	**Sepsis Nonsurvivors**	**SIRS**	**Sepsis Survivors**	**Sepsis Nonsurvivors**
n	29	90	31	34	18	29	36	25
Age	65.8 ± 13.6	56.4 ± 19.2	68.8 ± 16.7	58.9 ±18.1	58.0 ± 18.8	52.3 ± 16.0	54.8 ± 13.1	58.7 ± 164.5
Gender Male	41.4%	58.9%	54.8%	67.6%	61.1%	62.1%	52.8%	56.0%
Race (B/W/O)	21/7/1	56/28/6	23/7/1	17/14/3	8/8/2	8/18/3	4/29/3	1/23/1
APACHE II	16.2 ± 7.6	15.0 ± 7.1	22.8 ± 7.8	15.7 ± 5.8	18.5 ± 7.9	19.6 ± 9.3	25.9 ± 6.7	33.0 ± 9.8
SOFA	4.4 ± 2.9	4.9 ± 2.5	7.0 ± 3.6	4.3 ± 2.7	5.0 ± 3.0	N/R	N/R	N/R
Temp	36.8 ± 1.1	38.1 ± 1.7	37.4 ± 1.7	38.6 ± 1.1	37.8 ± 18.0	37.3 ± 0.9	38.3 ± 0.9	37.2 ± 1.9
MAP (mmHg)	89.3 ± 30.1	79.9 ± 19.1	69.0 ± 13.5	79.4 ±17.6	67.3 ± 14.9	71.5 ± 16.1	63.8 ± 11.4	65.7 ± 15.0
Sodium (mMol/L)	136.9 ± 4.4	136.1 ± 4.9	141.6 ± 10.6	138.0 ±4.4	136.2 ± 7.2	N/R	N/R	N/R
Hematocrit	34.8 ± 6.6	36.3 ± 6.6	30.6 ± 7.4	34.8 ± 5.7	32.4 ± 8.4	30.8 ± 6.7	28.3 ± 6.5	26.6 ± 5.5
Pathogen								
S. aureus	N/A	22	5	1	0	N/A	N/R	N/R
S. pneumoniae	N/A	25	6	2	1	N/A	N/R	N/R
E. coli	N/A	16	0	0	1	N/A	N/R	N/R
Comorbidities								
Alcohol abuse	17.2%	15.6%	12.9%	6.1%	5.9%	N/R	N/R	N/R
Neoplastic Disease	24.1%	6.7%	22.6%	20.6%	23.5%	24.1%	25.0%	76.0%
Diabetes	34.5%	34.4%	41.9%	23.5%	58.8%	31.0%	27.8%	8.0%
Congestive heart Failure	3.4%	6.7%	16.1%	6.6%	6.6%	0.0%	5.6%	0.0%
Chronic kidney disease	31.0%	22.2%	22.6%	17.6%	23.5%	6.9%	22.2%	36.0%
Chronic liver disease	6.9%	4.4%	19.4%	2.9%	0.0%	3.4%	8.3%	8.0%
Immunosuppression	3.4%	5.6%	6.5%	20.0%	15.0%	3.4%	16.7%	36.0%
Smoker	17.2%	28.9%	25.8%	17.6%	23.5%	20.7%	8.3%	16.0%

Data presented as mean ± standard deviation; RoCI - Registry of Critical Illness; B/W/O - black/white/other; N/R - not reported; N/A – not applicable.

Table 2

Predictive modeling of sepsis outcomes

	APACHE II (≥ 25)		
	Accuracy	**PPV**	**NPV**
t_0	77.2%	90.0%	36.4%
t_{24}	79.1%	87.3%	56.5%
Vt_0	73.9%	93.9%	23.1%
Vt_{24}	75.6%	96.7%	18.2%

	SOFA (≥ 7)		
	Accuracy	**PPV**	**NPV**
t_0	68.5%	70.0%	63.6%
t_{24}	65.2%	64.3%	66.7%
Vt_0	61.8%	75.0%	30.0%
Vt_{24}	47.6%	62.5%	38.5%

	Blood Lactate (≥ 4.0 mg/dL)		
	Accuracy	**PPV**	**NPV**
t_0	75.0%	90.8%	37.0%
t_{24}	61.2%	85.7%	20.0%
Vt_0	60.6%	85.7%	16.7%
Vt_{24}	75.0%	100.0%	25.0%

	Logistic Regression[1]				
	Accuracy	**AUC**	**RMSE**	**PPV**	**NPV**
t_0	85.1%	0.847	35.2%	94.4%	58.1%
t_{24}	79.8%	0.805	39.4%	85.9%	64.3%
Vt_0	74.5%	0.625	45.2%	94.1%	35.3%
Vt_{24}	77.1%	0.674	44.7%	93.8%	43.8%

	Logistic Regression[1]				
	Accuracy	**AUC**	**RMSE**	**PPV**	**NPV**
RoCI	71.7%	0.734	44.8%	91.4%	44.0%
QTA[1,2]	79.8%	0.767	39.6%	94.0%	43.0%
SVM[1,3] training	80.8%	0.819		86.4%	66.4%
SVM[1,3] test	74.6%	0.740		83.6%	55.0%

Root Mean Square Error (RMSE); positive predictive value (PPV; sepsis survivors prediction); negative predictive value (NPV; sepsis nonsurvivor prediction).

[1] 4-cis-decenoylcarnitine, 2-methylbutyroylcarnitine, butyroylcarnitine, hexanoylcarnitine, lactate, age, hematocrit.

[2] Quantitative targeted assays (QTA). 328 targeted assay values tested. All test sets and timepoints combined. Sepsis nonsurvivors, n= 93; sepsis survivors, n= 235.

[3] SVM (Support Vector Machine) utilizing QTA results. 173 unique sepsis survivors (n=124) and sepsis nonsurvivors (n=49); 87 for training, 86 for test. 100 iterations. Clinical lactate values were utilized. Unreported lactate values imputed from semi-quantitative data.